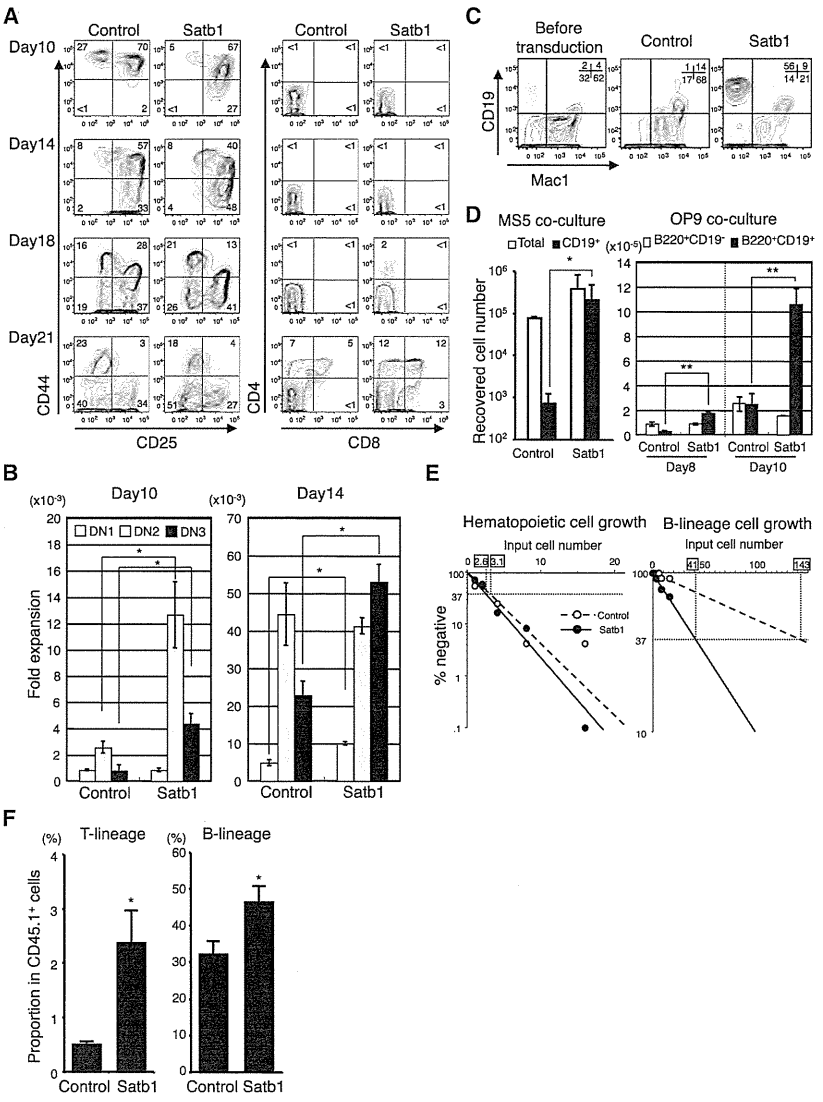

Figure 4. Satb1 Overexpression Promotes Lymphopoiesis

LSK Flt3$^-$ cells obtained from WT BM were retrovirally transduced with either a fluorescence-alone expressing control or a native Satb1 combined with GFP expressing vector. Successfully transduced cells were cultured, and their differentiation and proliferation were analyzed at the indicated period.

(A and B) Time-course analyses were performed for T-lineage cell generation in the OP9-DL1 coculture. Absolute numbers of recovered cells were divided by the numbers of transduced LSK Flt3$^-$ cells used to initiate the cultures to obtain the fold expansion values. Data are shown as mean ± SE.

(C) CD19 and Mac1 profiles are shown for cells recovered from MS5 cocultures on day 10. The left panel shows data obtained from fresh LSK Flt3$^-$ cells that did not undergo the retroviral infection.

(D) The absolute numbers of total recovered cells and B-lymphoid cells in the MS5 coculture (left panel). The output of B220$^+$ CD19$^-$ or B220$^+$ CD19$^+$ B-lineage cells was evaluated in the OP9 coculture (right panel). Cultures were established in triplicate. Data are shown as mean ± SE. Statistical significance is $^*p < 0.05$, $^{**}p < 0.01$.

(E) Limiting-dilution analyses were performed to determine the frequencies of hematopoietic progenitors that could give rise to CD19$^+$ B-lineage cells. Input cell numbers corresponding to each 37% negative value are shown in rectangles.

(F) One thousand LSK Flt3$^-$ cells (CD45.1) transduced with either Satb1-expressing or control vectors were transplanted to lethally irradiated WT mice (CD45.2) with 1 × 10^5 adult BM cells (CD45.2). Two weeks after transplantation, peripheral blood was collected to determine the proportion of CD4/CD8$^+$ T lineage and CD19$^+$ B lineage in CD45.1$^+$ cells. Data are shown as mean ± SE. Statistical significance is $^*p < 0.05$. (n = 5 in each group) (Figure 4, see also Figure S3).

their numbers were also enhanced by Satb1 overexpression (Figure S3F). Interestingly, the same Satb1-transduced LSKs differentiated to neither conventional nor plasmacytoid dendritic cells (Figure S3G).

The results from in vitro bulk cultures and assessment of lymphoid lineage cell numbers might reflect enhanced survival of lymphoid progenitors rather than priming or expansion of lymphoid potential in individual clones. Notably, no obvious increase in apoptotic cells occurred in any tested cultures with *Satb1*$^{-/-}$ cells or *Satb1*$^{-/-}$ lymphopoietic organs (data not shown and Figure S3H). Additionally, Satb1 overexpression conferred growth advantages to hematopoietic progenitors without influencing their viability in any of the cultures we used (data not shown). To investigate further the mechanisms through which Satb1 exerts its effect on early progenitors, we performed limiting dilution assays. On average, 1 in 3.1 control cells and 1 in 2.6 Satb1-transduced cells gave rise to blood cells, indicating that both are highly potent progenitors for hematopoietic cell growth (Figure 4E, left). Nevertheless, we observed significant differences between them regarding the frequencies of progenitors with lymphopoietic potential. While 1 in 41 Satb1-transduced Flt3$^-$ LSK cells produced B cells, only 1 in 143 control cells were lymphopoietic under these conditions (Figure 4E, right). In the same experiment, fresh Flt3$^-$ LSK cells without retroviral transfection produced hematopoietic cells and B cells at a frequency of 1 in 6.7 cells and 1 in 61 cells, respectively (data not shown).

These results suggest that Satb1 expression affects early lineage decisions in individual HSC and expands the growth and differentiation of lymphoid cells in vitro. To evaluate whether these findings were of practical value, we performed in vivo transplantation experiments with SATB1-transduced LSK Flt3$^-$ cells. We observed enhanced contribution of the SATB1-transduced cells to both T and B lineages in short-term engraftment (Figure 4F). To assess whether the overexpression of SATB1 induces tumors, we evaluated long-term and short-term

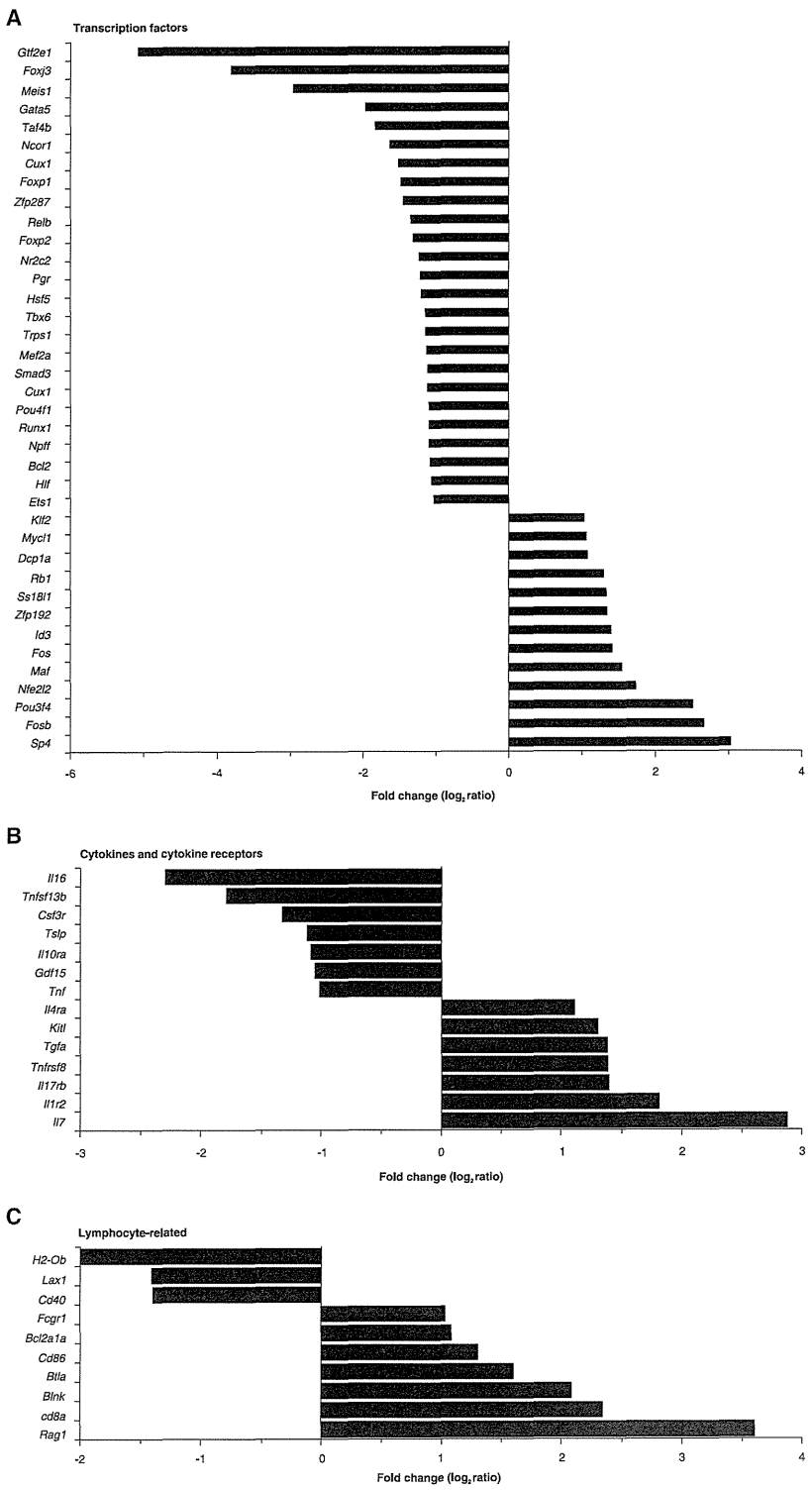

Figure 5. Genes Affected by Satb1 Expression

A microarray experiment was performed to compare gene expression in Satb1 and control-transduced LSK Flt3$^-$ cells. Upregulation in Satb1-transduced cells is shown as positive in each figure. (A) Transcription factors, (B) cytokine and cytokine receptors, and (C) other lymphoid lineage-related genes are summarized (Figure 5; see also Tables S2 and S3).

Satb1 Regulates Lymphoid Lineage-Related Genes in HSC

During early lymphocyte differentiation, several transcription factors have been shown to play roles in a hierarchical manner. To identify the target genes of Satb1, we first examined whether the exogenous expression of Satb1 influences the expression of lineage-relevant transcription factors in LSK Flt3$^-$ cells. Although high Satb1 expression was achieved, no significant upregulation was observed in the expression of *Sfpi1*, *Ikzf1*, *Tcf3*, or *Notch1* (data not shown). The expression of *Cebpa*, which is important for myeloid differentiation, was also not significantly affected (data not shown).

Next, to find candidate genes involved in the Satb1 induction of lymphopoiesis, we performed a microarray comparing gene expression between Satb1- and control-transduced LSK Flt3$^-$ cells (Table S2). In accordance with the results described above, the data showed no significant changes in the expression of *Sfpi1*, *Ikzf1*, *Tcf3*, *Notch1*, or *Cebpa*. However, several transcription factors involved in lymphoid differentiation, *Sp4*, *Maf*, *Fos*, and *Id3*, were upregulated in Satb1-transduced cells (Figure 5A). Cytokines such as *Il7* and *Kitl*, which are critical for lymphocyte differentiation and generally believed to be stromal cell products, were induced in hematopoietic progenitor cells themselves by ectopic expression of Satb1 (Figure 5B). While receptors for IL-4 or IL-17 were induced, *Csf3r*, encoding the G-CSF receptor, was downregulated. Interestingly, among lymphoid-related genes, *Rag1*, which is indispensable for both T and B cell differentiation, was strongly induced by Satb1 (Figure 5C). Expression of the CD86 gene that correlates with lymphoid competency (Shimazu et al., 2012) was also significantly elevated.

lymphohematopoiesis after transplantation. In eight transplanted mice, SATB1-overexpressing cells did not induce tumors, at least during 3 months of observation.

As a complementary experiment, we performed a set of microarray analyses comparing gene expression signatures between WT and *Satb1*$^{-/-}$ cells (Table S3). We again observed no direct correlations between Satb1 expression and *Ikzf1*, *Tcf3*, or *Notch1*, but confirmed that the expression of numerous lineage-related genes was influenced. The expression of *Il7* and *Kitl* was detectable in WT hematopoietic progenitors, and their levels were significantly lower in the *Satb1*$^{-/-}$ progenitors. Of note, *Satb2*, which is a homolog of *Satb1*, as well as *Bright*, which codes a B cell-specific AT-rich sequence binding protein (Herrscher et al., 1995), were upregulated in *Satb1*$^{-/-}$ HSC. In addition, the *Satb1*$^{-/-}$ HSC aberrantly expressed *Rag1* and *Pax5*, whose levels decreased with differentiation to LMPP. These results indicate that Satb1 expression globally influences many genes involved in lineage-fate decisions during the specification of HSC toward lymphoid lineages.

Satb1 Induces Lymphopoiesis in ESCs

Next, we examined whether the exogenous expression of Satb1 is sufficient to promote lymphopoiesis in ESCs. In the OP9 coculture system (Nakano et al., 1994), ESCs can produce mesoderm cells in 4.5 days, which have potential to become hematopoietic and endothelial cells. After a short period of retroviral transduction with the control-GFP or the Satb1-GFP vector, ES-derived mesoderm cells were cultured with OP9 in the presence of SCF, Flt3-ligand, and IL-7. As shown in Figure 6A, although both control- and Satb1-transfected cells contained substantial numbers of GFP$^+$ cells, the latter produced CD45$^+$ hematopoietic cells efficiently. Further phenotype revealed that most of the CD45$^+$ GFP$^+$ cells produced from the Satb1-transfected cells expressed B220 and CD19 (Figure 6A, right panels). Notably, those cells were also positive for AA4.1, CD11b, and CD5, suggesting that they were likely B1-B-lineage cells (Figure 6B).

Next, we established ESC clones, which can be induced to express Satb1-GFP on removal of tetracycline (Tet) from the culture medium. Eight days after Tet deprivation (day 12.5; Figure 6C), approximately 15% of the recovered cells were GFP$^+$ (data not shown). Thirty-five percent of these cells expressed CD45 and included substantial numbers of AA4.1$^+$ CD19$^+$ B-lineage cells (Figure 6D, right panels). Conversely, in the presence of Tet, the proportions of AA4.1$^+$ and CD19$^+$ cells among the CD45$^+$ faction were very low (Figure 6D, left panels). A majority of the CD19$^+$ cells among the Satb1-GFP$^+$ ES-derived cells were positive for Mac1 or CD5, again indicating a preference for the B1-B lineage (Figure 6E). In cytospin preparations, many of the ES-derived cells cultured with Tet showed myelomonocytic morphology, whereas Satb1/GFP$^+$ cells exhibited lymphocyte-like morphology (Figure 6F). Finally, a PCR-based *Igh* rearrangement assay confirmed D_H-J_H recombination in the Satb1-GFP$^+$ ES-derived cells (Figure 6G).

To test T-lineage potential, we transduced the control-GFP or the Satb1-GFP vector to ES-derived mesoderm cells and cultured them with OP9-DL1 cells. The Satb1-transduced cells effectively produced CD4$^+$ CD8$^+$ DP cells with rapid kinetics (Figures 6H and 6I). Substantial numbers of ES-derived T-lineage cells expressed TCR-γδ or TCR-β, and Satb1-transduced cells were advanced in this regard (data not shown). Taking these results together, we conclude that Satb1 expression directs even ES-derived cells toward lymphoid lineages.

Ectopic Satb1 Expression in Aged HSC Restores Lymphopoietic Potency

As shown in Figure 1B, the *Satb1* expression in HSC declines with age. This decline might be correlated with the age-dependent impairment of lymphopoiesis. Therefore, we examined whether Satb1 expression restores the lymphopoietic activity of progenitors from aged mice. Rag1-GFP$^-$ LSK cells of 2-year-old mice were transduced with control or Satb1-DsRed vectors. After 72 hr of transduction, DsRed$^+$ cells were sorted and cultured on OP9 in the presence of SCF, Flt3-ligand, and IL-7. The Satb1-transduced cells produced a percentage of Rag1-GFP$^+$ B220$^+$ cells that was significantly higher than that of control cells (Figure 7A). Indeed, most of the aged Rag1-GFP$^-$ LSK cells were prone to differentiate into Rag1-GFP$^+$ cells as a result of exogenous Satb1 expression. With respect to the recovered B-lineage cell counts, approximately 3-fold more B220$^+$ Rag1-GFP$^+$ Mac1$^-$ cells were obtained through Satb1 overexpression (Figure 7B).

Conversely, fewer B-lineage cells were generated from aged ELP than from young ELP despite their similar expression of *Satb1* (Figure 1B; Figure S4A). B-lineage differentiation of aged ELP also showed decreased Rag1 expression (Figure S4B). Nonetheless, aged ELP showed substantial lymphopoietic activity in MS5 cocultures, in which aged HSC scarcely produced B-lineage cells (Figure S4A). These results suggest that the downregulation of Satb1 expression is involved in the compromised lymphopoietic potential of aged HSC and that ectopic induction of Satb1 can at least partially restore the activity.

DISCUSSION

Despite accumulating evidence that multiple transcription factors support lymphocyte differentiation, ones that specifically direct HSC to the lymphoid lineage have remained elusive. One aim of this study was to describe molecular signatures of early stages of lymphopoiesis by comparing gene expression patterns between HSC and ELP. While we observed that many genes specific for the lymphoid lineage including *Tcr*, *Igh* and *Il7r* were highly induced at the ELP stage, some lymphoid genes were already expressed at low levels in the HSC-enriched fraction. Among them, we were particularly interested in chromatin modifiers because of their ability to control spatial and temporal expression of essential genes. Our screen identified Satb1, whose expression was previously linked to T lymphocyte differentiation (Alvarez et al., 2000). We show that Satb1 plays a critical role in directing HSC to lymphoid lineages.

Satb1 was originally identified as a protein that binds specifically to genomic DNA in a specialized DNA context with high base-unpairing potential (termed base-unpairing regions; BURs) (Dickinson et al., 1992). Satb1 is predominantly expressed in the thymus and subsequent studies revealed critical roles in thymocyte development (Alvarez et al., 2000), T cell activation (Cai et al., 2006), and Th2 differentiation (Notani et al., 2010). In thymocyte nuclei, Satb1 has a cage-like distribution and tethers BURs onto its regulatory network, thus organizing 3-dimensional chromatin architecture (Cai et al., 2003). By recruiting chromatin modifying and remodeling factors, Satb1 establishes region-specific epigenetic status at its target gene loci and regulates a large number of genes (Yasui et al., 2002;

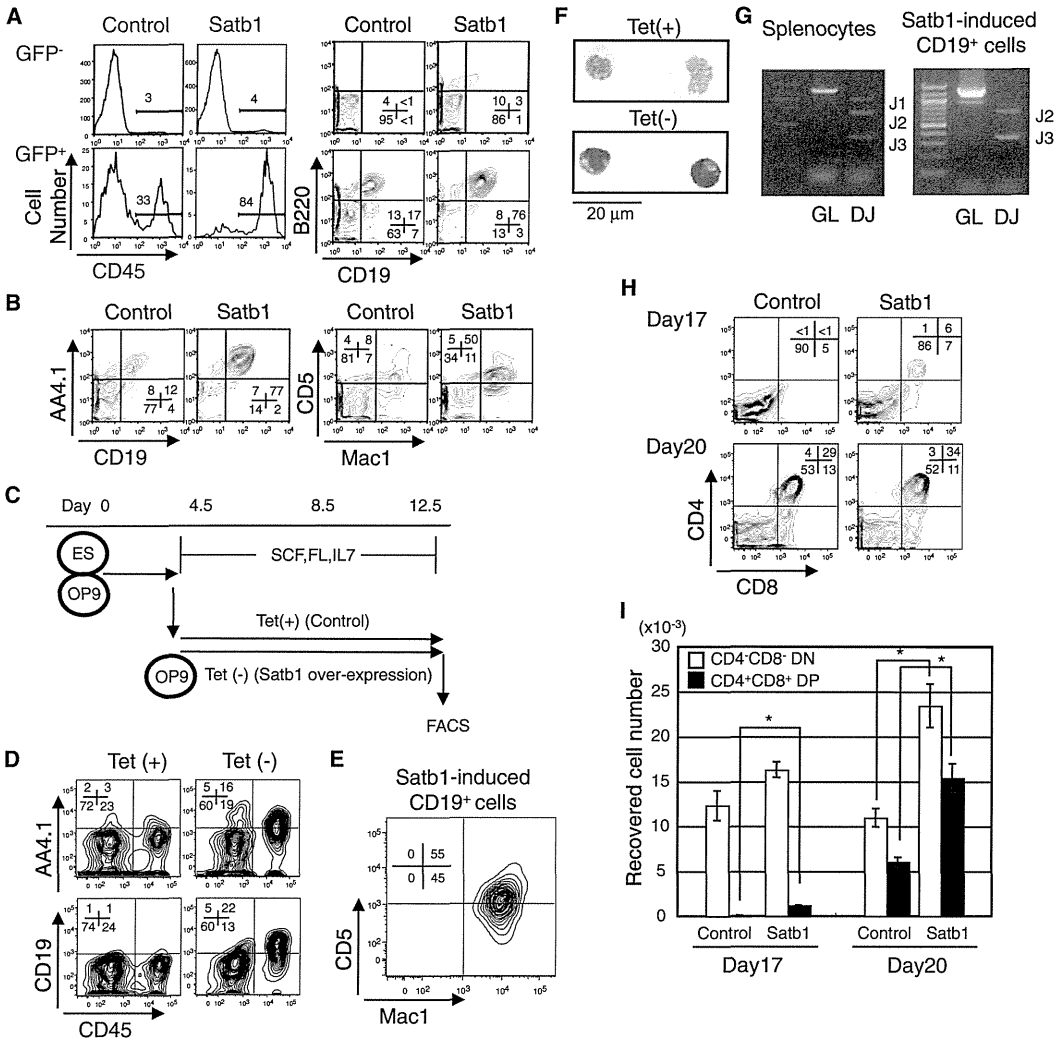

Figure 6. Satb1 Promotes Lymphoid Differentiation from ES-Derived Cells

E14tg2a ESCs were deprived of leukemia inhibitory factor and seeded onto OP9 cells. After 4.5 days, the differentiated mesoderm cells were infected with retroviral supernatants containing control-GFP or Satb1-GFP expressing vectors. Subsequently, the cells were cultured on OP9 for 8 days. At the end of culture, all cells were harvested and stained with the antibodies indicated in each panel.

(A) Total recovered cells were divided according to GFP expression (left panels). The percentages of $CD45^+$ cells in GFP^- (upper panels) and GFP^+ populations (lower panels) are shown. CD45R/B220 and CD19 profiles of the $CD45^+$ cells corresponding to the left panels (right panels) are shown.

(B) Representative AA4.1 and CD19 or Mac1 and CD5 profiles of the GFP^+ $CD45^+$ cells recovered from control or Satb1-transduced culture.

(C) The experimental design used with a Tet-off system (upper panel). ESCs, which inducibly express Satb1 by Tet deprivation, were established. After 4.5 days of culture without leukemia inhibitory factor in the presence of Tet, the differentiated cells were reseeded onto new OP9 stromal cells with or without Tet. Subsequently, FACS analysis was performed after 8 days of culture (day 12.5).

(D) Tet (+) indicates profiles of GFP^- cells cultured with Tet (left panels). Tet (–) panels show profiles of Satb1/GFP^+ cells cultured without Tet (right panels).

(E) Mac1 and CD5 expression on the Satb1/GFP^+ $CD19^+$ cells grown without Tet.

(F) Morphology of ES-derived hematopoietic cells on day 12.5.

(G) DNA PCR assays of germline (GL) or D_H-J_H rearranged *Igh* chain (DJ) genes were performed with the Satb1/GFP^+ $CD19^+$ cells recovered without Tet (right panel). Splenocytes were used as a positive control for the D_H-J_H recombination (left panel). On each gel, a size marker was loaded in the left lane.

(H and I) E14tg2a ESCs were differentiated to mesoderm cells for 4.5 days and then infected with the retroviral supernatant containing control-GFP or Satb1-GFP expressing vectors for 3 days. Subsequently, the cells were cultured on OP9-DL1 and T-lineage output was evaluated on the indicated days. Data are shown as mean ± SE. Statistical significance is $*p < 0.05$.

Cai et al., 2003). Increased Satb1 expression in hematopoietic progenitors compared with HSC has been observed by others (Forsberg et al., 2005; Ng et al., 2009); however, no study has been conducted concerning the role of Satb1 in differentiation of HSC to either lymphoid or myeloid progenitors. Our results clearly show a tight association of Satb1 expression with

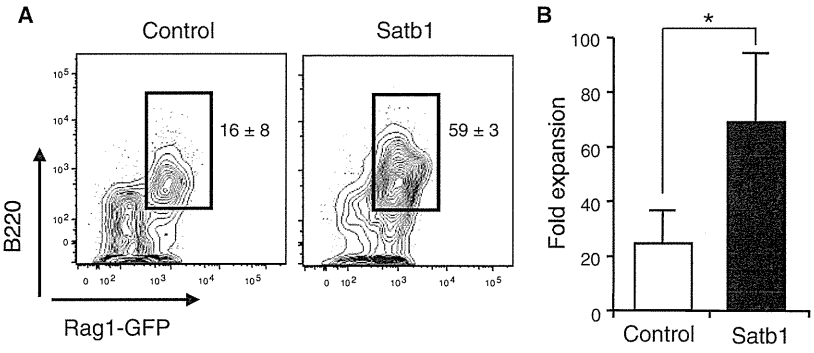

Figure 7. Satb1 Overexpression Restores Lymphopoietic Activity of Aged HSC
(A) Rag1/GFP$^-$ LSK cells were sorted from 2-year-old mice and retrovirally transduced with control or Satb1-DsRed vectors. Successfully transfected cells were cultured on OP9 cells. Cultures were established in triplicate. Numbers in each panel indicate the frequency of Rag1/GFP$^+$ CD45R/B220$^+$ cells.
(B) Yields of CD45R/B220$^+$ Rag1/GFP$^+$ Mac1$^-$ B-lineage cells per 1 input control- or Satb1-transduced Rag1/GFP-LSK cells were calculated and given as averages with SD bars. Statistical significance is *$p < 0.05$ (Figure 7; see also Figure S4).

lymphoid lineages even at the earliest stages. In addition, *Satb1*$^{-/-}$ HSCs are hindered in producing lymphocytes in vitro and in vivo that are consistent with the phenotypes originally described in *Satb1*$^{-/-}$ mice, suggesting an indispensable role of Satb1 in physiological lymphopoiesis.

Although we have previously identified molecules regulating early lymphoid differentiation, information about ones that initiate the process has been elusive (Oritani et al., 2000; Yokota et al., 2003b, 2008). The present study demonstrates that ectopic expression of Satb1 strongly induces differentiation toward lymphoid lineages and promotes lymphocyte growth from primitive progenitors, even when they are derived from aged BM or ESCs. We believe that these findings are important because they reveal that the earliest step of lymphopoiesis is affected by a global chromatin organizer. In addition, our results suggest that Satb1 expression could be a useful biomarker of aging and be manipulated to reverse immunosenescence.

Lymphoid-fate decisions are not necessarily determined by a few transcription factors or cytokines that positively regulate the differentiation in a hierarchical manner. The process should involve "closed windows" and "open opportunities." Gene array studies comparing HSC and ELP have shown that various lymphoid-related genes appear to be synchronously upregulated in ELP, whereas stem cell-related or myeloid-related ones are downregulated. From these observations, we speculated that a master regulator is present and involved in the synchronicity along with the hierarchical factors; further, we focused on the function of SATB1 in this process. Our results show that once Satb1 is substantially expressed in HSCs, it regulates hundreds of genes, including *Rag1*, *Il7*, *kitl*, and *Csf3r*, which together determine the lymphoid lineage fate. Satb1 itself has the determinant role in regulating a set of genes to exhibit the phenotype that we observed in vitro and in vivo experiments.

Increasing Satb1 beyond physiologic levels in HSCs and ESCs strongly augmented B lymphopoiesis, while depleting Satb1 from HSC dominantly impaired T lymphopoiesis in vivo. Satb1 overexpression in HSCs by itself induces an expression profile that favors B cell production. Conversely, Satb1 deficiency might have disrupted the delicate balance of Satb1 and other BUR-binding proteins such as Satb2 or Bright. We detected minimum levels of *Satb2* and *Bright* expression in WT HSC, and their expression levels significantly increase with B-lineage differentiation (data not shown). Interestingly, both genes were aberrantly induced in Satb1-deficient HSC (Table S2). Satb2 has a binding specificity similar to that of Satb1, and its expression is more predominant in the B lineage than in the T lineage (Dobreva et al., 2003). In ESCs, Satb2 function is antagonistic to Satb1 in regulating some target genes (Savarese et al., 2009). Whether these BUR-binding proteins are antagonistic or sometimes function synergistically, depending on cell differentiation or lineage remains unknown. Further studies of their functional correlation could yield important information about gene regulation in T and B lymphopoiesis.

Although our data provide evidence of a lymphocyte-inductive role of Satb1, an important question remains; that is, what regulates Satb1 expression? Depletion of long-lived mature B cells rejuvenates B-lymphopoiesis in old mice, suggesting that age-associated accumulation of aged B cells seems to be sensed by HSCs or early progenitors in BM (Keren et al., 2011). It will be interesting to learn whether such environmental cues influence Satb1 expression in HSCs. New strategies for boosting lymphocyte regeneration or protecting this capability during aging might emerge from studies of Satb1-related molecular mechanisms.

EXPERIMENTAL PROCEDURES

Animals

Animal studies were performed with the approval of the Institutional Review Board of Osaka University. Rag1-GFP knockin mice were previously described (Kuwata et al., 1999). *Satb1*$^{-/-}$ mice were also previously established (Alvarez et al., 2000). WT C57BL/6 mice and the congenic C57BL/6SJL strain (CD45.1 alloantigen) were obtained from Japan Clea (Shizuoka, Japan) and The Jackson Labs (Bar Harbor, ME), respectively. To obtain mouse fetuses, we considered the morning of the day of vaginal plug observation as E0.5.

Flow Cytometry and Cell Sorting

Cells were stained with Abs indicated in each experiment and analyzed with FACScanto or FACSaria (BD Bioscience). Adult BM cells from Rag1-GFP heterozygotes were used to isolate Lin$^-$ c-kit^{hi} Sca-1$^+$ Flt3$^-$ Rag1-GFP$^-$ IL-7Rα$^-$ (HSC-enriched), Lin$^-$ IL-7Rα$^-$ c-kit^{hi} Sca-1$^+$ Flt3$^+$ Rag1-GFP$^-$ (LMPP-enriched), Lin$^-$ IL-7Rα$^-$ c-kit^{hi} Sca-1$^+$ Flt3$^+$ Rag1-GFP$^+$ (ELP-enriched), Lin$^-$ c-kit^{lo} Sca-1^{lo} Flt3$^+$ Rag1-GFP$^+$ IL-7Rα$^+$ (CLP-enriched), and Lin$^-$ c-kit^{hi} Sca-1$^-$ IL-7Rα$^-$ myeloid progenitors (Adolfsson et al., 2005; Igarashi et al., 2002; Kondo et al., 1997). For culture experiments, we also sorted a HSC-enriched fraction from WT C57BL/6 or *Satb1*$^{-/-}$ mice according to the cell surface phenotype of Lin$^-$ c-kit^{hi} Sca-1$^+$ Flt3$^-$.

Stromal Cell Coculture

Murine stromal cell lines MS5 and OP9 were generous gifts from Dr. Mori (Niigata University) and Dr. Hayashi (Tottori University), respectively. Freshly

isolated or transduced cells were cocultured with stromal cells in α-MEM supplemented with 10% FCS, rm SCF (10 ng/mL), rm Flt3-ligand (20 ng/mL), and rm IL-7 (1 ng/mL). The cultures were fed twice a week and maintained for the indicated periods in each experiment. OP9-DL1 cells originated by Dr. Kawamoto (Riken, Japan) were obtained from Riken Cell Bank (Tsukuba, Japan) and used to produce T-lineage cells. In this case, cells were cultured in the presence of rm Flt3-ligand (5 ng/mL) and rm IL-7 (1ng/mL) for 14 days, and rm Flt3-ligand (5 ng/mL) alone thereafter. At the end of culture, cells were counted and analyzed by flow cytometry.

Competitive Repopulation Assay

The CD45.1/CD45.2 system was adapted to a competitive repopulation assay. One thousand Flt3$^-$ LSK cells sorted from FL or BM of WT, Satb1 heterodeficient, or Satb1 homozygous-deficient mice (CD45.2) were mixed with 4×10^5 unfractionated adult BM cells obtained from WT C57BL/6-Ly5.1 (CD45.1) mice and were transplanted into C57BL/6-Ly5.1 mice lethally irradiated at a dose of 920 rad. At 8 weeks after transplantation, engraftment of CD45.2 cells was evaluated by flow cytometry.

Retrovirus Transfection

Murine Satb1 expression vector was purchased from OriGene (Rockville, MD). A retrovirus expression vector for Satb1 was generated by subcloning into the pMYs-IRES-GFP or DsRed vector (a gift from Dr. Kitamura, University of Tokoyo). Conditioned medium containing high tighter retrovirus particles was prepared as reported previously (Satoh et al., 2008). Sorted HSC were cultured in D-MEM containing 10% FBS, rm SCF (100 ng/ml), rm TPO (100 ng/ml), and rm Flt3-ligand (100 ng/ml) for 24 hr. Then, the cells were seeded into the culture plates coated with Retronectin (Takara Bio, Shiga, Japan) and cultured with conditioned medium containing retrovirus. After 24 hr, cells were washed and performed second transfection by the same condition. After 48 hr from the second transfection, GFP or DsRed-positive cells were sorted by FACSaria.

Limiting Dilution Assays

The frequencies of lymphohematopoietic progenitors were determined by plating cells in limiting dilution assays by using 96-well flat-bottom plates. Pre-established MS5 layers were plated with 1, 2, 4, 8, or 16 cells each by using the Automated Cell Deposition Unit of the FACSaria. Cells were cultured in α-MEM supplemented with 10% FCS, rm SCF (10 ng/mL), rm Flt3-ligand (20 ng/mL), and rm IL-7 (1 ng/mL). At 10 days of culture, wells were inspected for the presence of hematopoietic clones. Positive wells were harvested and analyzed by flow cytometry for the presence of CD45$^+$ hematopoietic cells and CD45R/B220$^+$ CD19$^+$ Mac1$^-$ B-lineage cells. The frequencies of progenitors were calculated by linear regression analysis on the basis of Poisson distribution as the reciprocal of the concentration of test cells that gave 37% negative cultures.

Lymphocyte Development from Murine ESCs

To induce differentiation toward hematopoietic cells, we deprived E14tg2a ESCs of leukemia inhibitory factor and seeded onto OP9 cells in 6-well plates at a density of 10^4 cells per well in α-MEM supplemented with 20% FBS (Nakano et al., 1994). After 4.5 days, the cells were harvested and whole-cell suspensions were transferred into a new 10 cm dish and incubated in 37°C for 30 min to remove adherent OP9 cells. The collected floating cells were infected with the retroviral supernatant in Retronectin-coated plates by 2 hr spinoculation (1100 *g*) (Kitajima et al., 2006). Subsequently, the cells were cultured on OP9 or OP9-DL1.

Tetracycline-Regulated Inducible Expression of Satb1 in ESCs

To inducibly express Satb1 in ESCs, we utilized a Tet-off system as reported previously (Era and Witte, 2000), in which transcription of the target gene is initiated by the removal of Tet from the culture medium. Briefly, we initially introduced pCAG20-1-tTA and pUHD10-3-puro by electroporation and selected one clone designated E14 by culture with 1 μg/ml of Puro and/or 1 μg/ml of Tet. We further transfected pUHD10–3-Satb1-GFP, which can inducibly express Satb1 and GFP as a single mRNA through the internal ribosome entry site in response to the Tet removal, together with the neomycin-resistant plasmid pcDNA3.1-neo. After the culture with G418, we selected clones that can inducibly express GFP in response to the Tet deprivation.

DNA PCR Assays for *Igh* Rearrangement

DNA PCR assays were performed as reported previously (Schlissel et al., 1991). PCR was performed by using genomic DNA extracted from splenocytes or ES-derived cells as a template. D_H-J_H recombination was detected as amplified fragments of 1,033 bp, 716 bp, and 333 bp by using a primer $D_HL(5')$ and J3(3′). Germline alleles were detected as an amplified fragment of 1,259 bp by using a primer Mu0(5′) and J3(3′). The sequence of primers are as follows: $D_HL(5')$, GGAATTCG(AorC)TTTTTGT(CorG)AAGGGATCTACTA CTGTG; Mu0(5′), CCGCATGCCAAGGCTAGCCTGAAAGATTACC; and J3(3′), GTCTAGATTCTCACAAGAGTCCGATAGACCCTGG.

Statistical Analyses

Unpaired, two-tailed t test analyses were used for intergroup comparisons, and p values were considered significant if they were less than 0.05.

ACCESSION NUMBERS

The microarray data in Tables S2 and S3 has been deposited in NCBI GEO database under the accession numbers GSE45566 and GSE45299.

SUPPLEMENTAL INFORMATION

Supplemental Information includes four figures, three tables, and Supplemental Experimental Procedures and can be found with this article online at http://dx.doi.org/10.1016/j.immuni.2013.05.014.

ACKNOWLEDGMENTS

We thank T. Nakano for discussion of the results. This work was supported in part by a grant from Mitsubishi Pharma Research Foundation and grants AI020069, HL107138-03, and R37 CA039681 from the National Institutes of Health.

Received: August 30, 2011
Accepted: March 6, 2013
Published: June 20, 2013

REFERENCES

Adolfsson, J., Månsson, R., Buza-Vidas, N., Hultquist, A., Liuba, K., Jensen, C.T., Bryder, D., Yang, L., Borge, O.J., Thoren, L.A., et al. (2005). Identification of Flt3+ lympho-myeloid stem cells lacking erythro-megakaryocytic potential a revised road map for adult blood lineage commitment. Cell *121*, 295–306.

Alvarez, J.D., Yasui, D.H., Niida, H., Joh, T., Loh, D.Y., and Kohwi-Shigematsu, T. (2000). The MAR-binding protein SATB1 orchestrates temporal and spatial expression of multiple genes during T-cell development. Genes Dev. *14*, 521–535.

Cai, S., Han, H.J., and Kohwi-Shigematsu, T. (2003). Tissue-specific nuclear architecture and gene expression regulated by SATB1. Nat. Genet. *34*, 42–51.

Cai, S., Lee, C.C., and Kohwi-Shigematsu, T. (2006). SATB1 packages densely looped, transcriptionally active chromatin for coordinated expression of cytokine genes. Nat. Genet. *38*, 1278–1288.

Chambers, S.M., Shaw, C.A., Gatza, C., Fisk, C.J., Donehower, L.A., and Goodell, M.A. (2007). Aging hematopoietic stem cells decline in function and exhibit epigenetic dysregulation. PLoS Biol. *5*, e201.

Dias, S., Månsson, R., Gurbuxani, S., Sigvardsson, M., and Kee, B.L. (2008). E2A proteins promote development of lymphoid-primed multipotent progenitors. Immunity *29*, 217–227.

Dickinson, L.A., Joh, T., Kohwi, Y., and Kohwi-Shigematsu, T. (1992). A tissue-specific MAR/SAR DNA-binding protein with unusual binding site recognition. Cell *70*, 631–645.

Dobreva, G., Dambacher, J., and Grosschedl, R. (2003). SUMO modification of a novel MAR-binding protein, SATB2, modulates immunoglobulin mu gene expression. Genes Dev. *17*, 3048–3061.

Era, T., and Witte, O.N. (2000). Regulated expression of P210 Bcr-Abl during embryonic stem cell differentiation stimulates multipotential progenitor expansion and myeloid cell fate. Proc. Natl. Acad. Sci. USA *97*, 1737–1742.

Forsberg, E.C., Prohaska, S.S., Katzman, S., Heffner, G.C., Stuart, J.M., and Weissman, I.L. (2005). Differential expression of novel potential regulators in hematopoietic stem cells. PLoS Genet. *1*, e28.

Han, H.J., Russo, J., Kohwi, Y., and Kohwi-Shigematsu, T. (2008). SATB1 reprogrammes gene expression to promote breast tumour growth and metastasis. Nature *452*, 187–193.

Herrscher, R.F., Kaplan, M.H., Lelsz, D.L., Das, C., Scheuermann, R., and Tucker, P.W. (1995). The immunoglobulin heavy-chain matrix-associating regions are bound by Bright: a B cell-specific trans-activator that describes a new DNA-binding protein family. Genes Dev. *9*, 3067–3082.

Igarashi, H., Gregory, S.C., Yokota, T., Sakaguchi, N., and Kincade, P.W. (2002). Transcription from the RAG1 locus marks the earliest lymphocyte progenitors in bone marrow. Immunity *17*, 117–130.

Ikawa, T., Kawamoto, H., Goldrath, A.W., and Murre, C. (2006). E proteins and Notch signaling cooperate to promote T cell lineage specification and commitment. J. Exp. Med. *203*, 1329–1342.

Keren, Z., Naor, S., Nussbaum, S., Golan, K., Itkin, T., Sasaki, Y., Schmidt-Supprian, M., Lapidot, T., and Melamed, D. (2011). B-cell depletion reactivates B lymphopoiesis in the BM and rejuvenates the B lineage in aging. Blood *117*, 3104–3112.

Kitajima, K., Tanaka, M., Zheng, J., Yen, H., Sato, A., Sugiyama, D., Umehara, H., Sakai, E., and Nakano, T. (2006). Redirecting differentiation of hematopoietic progenitors by a transcription factor, GATA-2. Blood *107*, 1857–1863.

Kondo, M., Weissman, I.L., and Akashi, K. (1997). Identification of clonogenic common lymphoid progenitors in mouse bone marrow. Cell *91*, 661–672.

Kuwata, N., Igarashi, H., Ohmura, T., Aizawa, S., and Sakaguchi, N. (1999). Cutting edge: absence of expression of RAG1 in peritoneal B-1 cells detected by knocking into RAG1 locus with green fluorescent protein gene. J. Immunol. *163*, 6355–6359.

Lai, A.Y., and Kondo, M. (2008). T and B lymphocyte differentiation from hematopoietic stem cell. Semin. Immunol. *20*, 207–212.

Medina, K.L., Pongubala, J.M., Reddy, K.L., Lancki, D.W., Dekoter, R., Kieslinger, M., Grosschedl, R., and Singh, H. (2004). Assembling a gene regulatory network for specification of the B cell fate. Dev. Cell *7*, 607–617.

Miller, J.P., and Allman, D. (2005). Linking age-related defects in B lymphopoiesis to the aging of hematopoietic stem cells. Semin. Immunol. *17*, 321–329.

Montecino-Rodriguez, E., and Dorshkind, K. (2006). Evolving patterns of lymphopoiesis from embryogenesis through senescence. Immunity *24*, 659–662.

Nakano, T., Kodama, H., and Honjo, T. (1994). Generation of lymphohematopoietic cells from embryonic stem cells in culture. Science *265*, 1098–1101.

Ng, S.Y., Yoshida, T., Zhang, J., and Georgopoulos, K. (2009). Genome-wide lineage-specific transcriptional networks underscore Ikaros-dependent lymphoid priming in hematopoietic stem cells. Immunity *30*, 493–507.

Notani, D., Gottimukkala, K.P., Jayani, R.S., Limaye, A.S., Damle, M.V., Mehta, S., Purbey, P.K., Joseph, J., and Galande, S. (2010). Global regulator SATB1 recruits beta-catenin and regulates T(H)2 differentiation in Wnt-dependent manner. PLoS Biol. *8*, e1000296.

Oritani, K., Medina, K.L., Tomiyama, Y., Ishikawa, J., Okajima, Y., Ogawa, M., Yokota, T., Aoyama, K., Takahashi, I., Kincade, P.W., and Matsuzawa, Y. (2000). Limitin: An interferon-like cytokine that preferentially influences B-lymphocyte precursors. Nat. Med. *6*, 659–666.

Rossi, D.J., Bryder, D., Zahn, J.M., Ahlenius, H., Sonu, R., Wagers, A.J., and Weissman, I.L. (2005). Cell intrinsic alterations underlie hematopoietic stem cell aging. Proc. Natl. Acad. Sci. USA *102*, 9194–9199.

Satoh, Y., Matsumura, I., Tanaka, H., Ezoe, S., Fukushima, K., Tokunaga, M., Yasumi, M., Shibayama, H., Mizuki, M., Era, T., et al. (2008). AML1/RUNX1 works as a negative regulator of c-Mpl in hematopoietic stem cells. J. Biol. Chem. *283*, 30045–30056.

Savarese, F., Dávila, A., Nechanitzky, R., De La Rosa-Velazquez, I., Pereira, C.F., Engelke, R., Takahashi, K., Jenuwein, T., Kohwi-Shigematsu, T., Fisher, A.G., and Grosschedl, R. (2009). Satb1 and Satb2 regulate embryonic stem cell differentiation and Nanog expression. Genes Dev. *23*, 2625–2638.

Schlissel, M.S., Corcoran, L.M., and Baltimore, D. (1991). Virus-transformed pre-B cells show ordered activation but not inactivation of immunoglobulin gene rearrangement and transcription. J. Exp. Med. *173*, 711–720.

Scott, E.W., Fisher, R.C., Olson, M.C., Kehrli, E.W., Simon, M.C., and Singh, H. (1997). PU.1 functions in a cell-autonomous manner to control the differentiation of multipotential lymphoid-myeloid progenitors. Immunity *6*, 437–447.

Semerad, C.L., Mercer, E.M., Inlay, M.A., Weissman, I.L., and Murre, C. (2009). E2A proteins maintain the hematopoietic stem cell pool and promote the maturation of myelolymphoid and myeloerythroid progenitors. Proc. Natl. Acad. Sci. USA *106*, 1930–1935.

Shimazu, T., Iida, R., Zhang, Q., Welner, R.S., Medina, K.L., Alberola-Lla, J., and Kincade, P.W. (2012). CD86 is expressed on murine hematopoietic stem cells and denotes lymphopoietic potential. Blood *119*, 4889–4897.

Sudo, K., Ema, H., Morita, Y., and Nakauchi, H. (2000). Age-associated characteristics of murine hematopoietic stem cells. J. Exp. Med. *192*, 1273–1280.

Yang, Q., Kardava, L., St Leger, A., Martincic, K., Varnum-Finney, B., Bernstein, I.D., Milcarek, C., and Borghesi, L. (2008). E47 controls the developmental integrity and cell cycle quiescence of multipotential hematopoietic progenitors. J. Immunol. *181*, 5885–5894.

Yasui, D., Miyano, M., Cai, S., Varga-Weisz, P., and Kohwi-Shigematsu, T. (2002). SATB1 targets chromatin remodelling to regulate genes over long distances. Nature *419*, 641–645.

Yilmaz, O.H., Kiel, M.J., and Morrison, S.J. (2006). SLAM family markers are conserved among hematopoietic stem cells from old and reconstituted mice and markedly increase their purity. Blood *107*, 924–930.

Yokota, T., Kouro, T., Hirose, J., Igarashi, H., Garrett, K.P., Gregory, S.C., Sakaguchi, N., Owen, J.J., and Kincade, P.W. (2003a). Unique properties of fetal lymphoid progenitors identified according to RAG1 gene expression. Immunity *19*, 365–375.

Yokota, T., Meka, C.S., Kouro, T., Medina, K.L., Igarashi, H., Takahashi, M., Oritani, K., Funahashi, T., Tomiyama, Y., Matsuzawa, Y., and Kincade, P.W. (2003b). Adiponectin, a fat cell product, influences the earliest lymphocyte precursors in bone marrow cultures by activation of the cyclooxygenase-prostaglandin pathway in stromal cells. J. Immunol. *171*, 5091–5099.

Yokota, T., Oritani, K., Garrett, K.P., Kouro, T., Nishida, M., Takahashi, I., Ichii, M., Satoh, Y., Kincade, P.W., and Kanakura, Y. (2008). Soluble frizzled-related protein 1 is estrogen inducible in bone marrow stromal cells and suppresses the earliest events in lymphopoiesis. J. Immunol. *181*, 6061–6072.

Yoshida, T., Ng, S.Y., Zuniga-Pflucker, J.C., and Georgopoulos, K. (2006). Early hematopoietic lineage restrictions directed by Ikaros. Nat. Immunol. *7*, 382–391.

Increased plasma thrombopoietin levels in patients with myelodysplastic syndrome: a reliable marker for a benign subset of bone marrow failure

Yu Seiki, Yumi Sasaki, Kohei Hosokawa, Chizuru Saito, Naomi Sugimori, Hirohito Yamazaki, Akiyoshi Takami, and Shinji Nakao

Cellular Transplantation Biology, Kanazawa University Graduate School of Medical Science, Kanazawa, Japan

ABSTRACT

Although myelodysplastic syndromes are heterogeneous disorders comprising a benign subset of bone marrow failure similar to aplastic anemia, no laboratory test has been established to distinguish it from bone marrow failures that can evolve into acute myeloid leukemia. Plasma thrombopoietin levels were measured in 120 patients who had myelodysplastic syndrome with thrombocytopenia (< 100 x 10^9/L) to determine any correlation to markers associated with immune pathophysiology and outcome. Thrombopoietin levels were consistently low for patients with refractory anemia with excess of blasts, while patients with other myelodysplatic syndrome subsets had more variable results. Patients with thrombopoietin levels of 320 pg/mL and over had increased glycosylphosphatidylinositol-anchored protein-deficient blood cells (49.1% *vs.* 0%), were more likely to have a low International Prognostic Scoring System (IPSS) score (≤1.0, 100% *vs.* 65.5%), a higher response rate to immunosuppressive therapy (84.2% *vs.* 14.3%), and a better 5-year progression-free survival rate (94.1% *vs.* 63.6% for refractory cytopenia with unilineage dysplasia; 100.0% *vs.* 44.4% for refractory cytopenia with multilineage dysplasia). In conclusion, increased plasma thrombopoietin levels were associated with a favorable prognosis of bone marrow failure and could, therefore, represent a reliable marker for a benign subset of myelodysplastic syndrome.

Introduction

Myelodysplastic syndromes (MDS) are characterized by peripheral cytopenia and morphological abnormalities in mature and immature blood cells. Although MDS were originally defined as clonal hematopoietic disorders with a propensity to become acute myeloid leukemia (AML), they also comprise benign bone marrow (BM) failure which may benefit from immunosuppressive therapy (IST), as acquired aplastic anemia (AA) does.[1-3] MDS with thrombocytopenia are often difficult to differentiate from non-severe AA because diagnoses rely on a subjective judgment of blood cell morphological abnormalities, and BM cellularity is often inconsistent among the sites examined.[4,5] Laboratory markers such as glycosylphosphatidylinositol-anchored protein-deficient (GPI-AP$^-$) cells and HLA-DRB1*1501 may differentiate between benign and pre-leukemic MDS subtypes.[6,7] Diagnostic values of these markers have not been established, however, due to conflicting results in the prediction of IST response[8] and cumbersome procedures in the detection of minor GPI-AP$^-$ cell populations.[9,10]

Thrombocytopenia is a symptom common to AA and a subset of MDS. Previous studies showed that plasma levels of thrombopoietin (TPO), a critical regulator of thrombopoiesis, were elevated in patients with AA[11] but remained low in patients with MDS despite the presence of severe thrombocytopenia.[12-14] The low TPO levels in MDS patients have been connected to an increase in megakaryocytes or TPO receptors on megakaryocytes,[13] but no studies have focused on the possibility of different TPO levels among MDS subtypes. Patients with low-risk MDS could have high TPO levels and respond to IST as AA patients do. To test these hypotheses, plasma TPO was measured in patients with various types of MDS and correlated to IST response, patient prognosis and an increase in the percentage of GPI-AP$^-$ cells.

Design and Methods

Patients' characteristics

TPO plasma concentration was measured in 50 healthy volunteers (23 male, 27 female) aged 18-82 years old (median 41 years) and 191 patients diagnosed with thrombocytopenia from 2005 to 2010 at Kanazawa University Hospital, hospitals participating in the Study Group of Intractable Hematopoietic Disorders in Japan, or other affiliated institutions. There were 120 patients with MDS, including 37 with refractory cytopenia with unilineage dysplasia (RCUD), 40 with refractory cytopenia with multilineage dysplasia (RCMD), 22 with refractory anemia with excess of blasts (RAEB), and 21 with unclassified MDS (MDS-U), as well as 47 patients with AA and 24 with immune thrombocytopenia (ITP). Characteristics of these participants are summarized in Table 1. Patients dependent on platelet transfusions or with a liver dysfunction were excluded from the study. AA and MDS were classified according to diagnostic criteria from the International Agranulocytosis and Aplastic Anemia Study Group and World Health Organization 2008, respectively. Prognostic sores of MDS patients were calculated according to the International Prognostic Scoring System (IPSS). AA severity was

 Haematologica 2013;98. doi:10.3324/haematol.2012.066217
The online version of this paper has a Supplementary Appendix.
Manuscript received on April 19, 2012. Manuscript accepted on December 19, 2012.
Correspondence: snakao@staff.kanazawa-u.ac.jp

determined by criteria from Camitta *et al.*[15] All patients with MDS were judged to have 30% or more marrow cellularity by pathologists. MDS-U patients with abnormal karyotypes included 15 with del(13q), 2 with del(1;7), one with del(11q), one with t(4;21)(q11;q11), one with trisomy 8, and one with del(20q). The patients with trisomy 8 and del(20q) were diagnosed with MDS-U by the presence of bicytopenia. The ethics committee of Kanazawa University Graduate School of Medical Science approved the study protocol, and all patients provided their informed consent prior to sampling.

Measurement of TPO levels

Ethylenediaminetetraacetic acid (EDTA)-anticoagulated whole blood was drawn from patients at diagnosis, and plasma was separated by centrifugation at 1000 g for 10 min for storage at -20°C. Plasma TPO was measured with a commercially available assay kit (Quantikine™ Human TPO Immunoassay, R&D Systems, Minneapolis, MN, USA) according to the manufacturer's instructions. Corrected TPO values were calculated by dividing TPO concentration by platelet count (x 10^9/L).

Detection of GPI-AP$^-$ blood cells

EDTA-anticoagulated peripheral blood was drawn from each patient. To detect GPI-AP$^-$ granulocytes, erythrocytes were lysed in buffer (8.26 g/L NH4Cl, 1.0 g/L KHCO3, and 0.037 g/L EDTA-4Na). After a saline wash, 50 μL of leukocyte suspension was incubated with 4 μL of phycoerythrin (PE)-labeled anti-CD11b mAb (Becton Dickinson, Franklin Lakes, NJ, USA) and 6 μL of Alex Fluor 488-labeled inactive toxin aerolysin (FLAER; Pinewood Scientific Services, Victoria, BC, Canada). To detect GPI-AP$^-$ erythrocytes, fresh blood was diluted to 3% in phosphate buffered saline (PBS), and 50 μL was then incubated with 4 μL of PE-labeled anti-glycophorin A mAb (clone JC159; DAKO, Glostrup, Denmark), fluorescein-isothiocyanate (FITC)-labeled anti-CD55 mAbs (clone IA10, mouse IgG2a; Pharmingen, San Diego, CA, USA), and FITC-labeled anti-CD59 mAbs (clone p282, mouse IgG2a; Pharmingen). At least 1 x 10^5 CD11b$^+$ granulocytes and glycophorin A$^+$ red blood cells (RBCs) were analyzed within each corresponding gate of a FACSCanto II® (Becton Dickinson) flow cytometer.[9] A significant increase in the percentage of GPI-AP$^-$ cells was defined as greater than 0.003% aerolysin-CD11b$^+$ granulocytes and/or greater than 0.005% glycophorin A$^+$ RBCs as determined from the peripheral blood of 50 healthy individuals. Careful handling of samples with elaborate gating could lower the cut-off values to these levels without producing false positive results.[9,16,17]

IST

Horse anti-thymocyte globulin (ATG) 15 mg/kg/d (Genzyme, Cambridge, MA, USA) was administered for five days in combination with cyclosporine A (CsA) 6 mg/kg/d (Novartis, Basel, Switzerland). CsA was also given at 5-6 mg/kg/d for at least three months as monotherapy. Hematologic improvements, partial response, and complete response were defined according to the International MDS Working Group Criteria.[18]

Human androgen receptor assay (HUMARA)

The androgen receptor gene was amplified from the genomic DNA of 8 female patients, as previously described by Ishiyama *et al.* with some modifications.[19] To correct an inequality of amplification efficiency between the 2 alleles, we determined the ratios of both allele areas before (lower allele/higher allele: A/B) and after (lower allele/higher allele:A'/B') HhaI digestion using a C value calculated by (A/B)/(A'/B') as a marker of skewing in granulocytes (CG) and T lymphocytes (CL). Skewing was judged evident when the absolute values of log (CG/CL) (S value) were more than 0.4.

Statistical analysis

Plasma TPO concentrations were compared between subgroups with different clinical characteristics using the Mann-Whitney U test. Receiver operating characteristic (ROC) curves were calculated from the TPO levels and corrected TPO values of AA patients (representing benign BM failure) and RAEB patients (representing pre-leukemic BM failure) to determine thresholds of plasma TPO levels and define patients with high TPO levels. ROC curves were also calculated from the TPO levels of patients with early stage MDS who responded to IST and those who did not respond, and of patients who progressed to AML/death and those who did not progress. The Kaplan-Meier method and Cox's proportional hazards model were performed to estimate time-to-event analysis. Differences between patients with TPO levels of 320 pg/mL or more (TPO^{high}) and patients with TPO levels less than 320 pg/mL (TPO^{low}) were assessed by the log rank test. The differences in the percentages of patients with low International Prognostic Scoring System (IPSS) scores and of patients requiring platelet transfusions between TPO^{high} and TPO^{low} patients were assessed by Fisher's exact probability test. All statistical analyses were performed using JMP version 5.0.1J software (SAS Institute, Cary, NC, USA). $P<0.05$ was considered significant.

Results

TPO levels for patients with thrombocytopenia

Plasma TPO levels ranged from 19.4 to 38.8 pg/mL (mean ± standard deviation, 54.5 ± 21.1 pg/mL) in healthy individuals with platelet counts higher than 150 x 10^9/L. Similar to previous reports, TPO levels for patients with AA (1254.6 ± 551.1 pg/mL) were noticeably higher than for patients with ITP (63.5 ± 8.7 pg/mL) or RAEB (44.7 ± 85.2 pg/mL) (Figure 1A). Corrected TPO values were also higher in AA patients than RAEB patients (Figure 1B). ROC curves set the threshold between benign and pre-leukemic BM failure at 320 pg/mL for TPO levels and 157 pg/mL/1010 L for corrected TPO values (Figure 2A). All patients with TPO levels of 320 pg/mL or over also had corrected TPO values over 157 pg/mL/10^{10}L, except one with 155 pg/mL/10^{10}L, indicating that the difference between TPO^{high} and TPO^{low} patients is not due to platelet

Table 1. **Characteristics of study participants with thrombocytopenia and healthy volunteers.**

	N. of patients	Sex, (M/F)	Age (years), (range)	Platelet count (x10^9/L) (median ± SE)
MDS	120	60/49	70 (19-91)	54.0 ± 2.7
RCUD	37	17/20	65 (46-85)	53.7 ± 4.3
RCMD	40	23/17	69 (33-91)	43.5 ± 8.2
RAEB	22	16/6	74 (43-85)	49.1 ± 2.7
MDS-U	21	10/11	72 (19-76)	62.2 ± 2.1
AA	47	25/22	58 (12-93)	24.9 ± 7.3
Severe	23	12/11	56 (28-93)	11.6 ± 6.9
Moderate	24	13/11	58 (12-83)	43.9 ± 5.4
ITP	24	14/10	62 (35-82)	23.5± 7.9
Healthy volunteers	50	23/27	41 (18-59)	304.3 ± 8.6

MDS: myelodysplastic syndrome; RCUD: refractory cytopenia with unilineage dysplasia; RCMD: refractory cytopenia with multilineage dysplasia; RAEB: refractory anemia with excess of blasts; MDS-U: unclassified myelodysplastic syndromes; AA: aplastic anemia; ITP: immune thrombocytopenia; HV: healthy volunteers.

count. TPO levels were highly variable in patients with MDS subtypes other than RAEB, with the proportion of TPOhigh patients at 40.5% for RCUD, 32.5% for RCMD, and 77.3% for MDS-U.

Prevalence of increased GPI-AP$^-$ cells, clonality, and IPSS scores for patients with MDS

Small populations of GPI-AP$^-$ granulocytes and/or erythrocytes were detected in some MDS patients, at 29.7% for RCUD, 7.5% for RCMD, 62.9% for MDS-U, and 0% for RAEB. Figure 3A shows the percentage of GPI-AP$^-$ granulocytes in 55 TPO^{high} (25 with RCUD, 14 with RCMD, and 16 with MDS-U) and 65 TPO^{low} (12 with RCUD, 26 with RCMD, 5 with MDS-U, and 22 with RAEB) patients. The prevalence of increased GPI-AP$^-$ granulocytes and/or erythrocytes in each group was 45.8% and 0% (P=0.003, Figure 3B). Eight female patients (4 with RCMD and 4 with MDS-U) underwent the HUMARA. All 4TPO^{low} patients showed S values over 0.4 (1.23, 1.39, 1.14, and 0.71) compatible with the presence of clonal hematopoiesis while none of the 4 TPO^{high} patients showed such high S values (0.06, 0.16, 0.08, and 0.09, P=0.002, *Online Supplementary Figure S1*). When correlation of TPO levels and IPSS scores was examined for each MDS patient, none of the TPO^{high} patients had an IPSS score above 1.5 (Figure 3C). In fact, the percentages of 0, 0.5, or 1.0 scores in TPO^{high} and TPO^{low} patient groups were 100.0% and 65.5%, respectively (P<0.001).

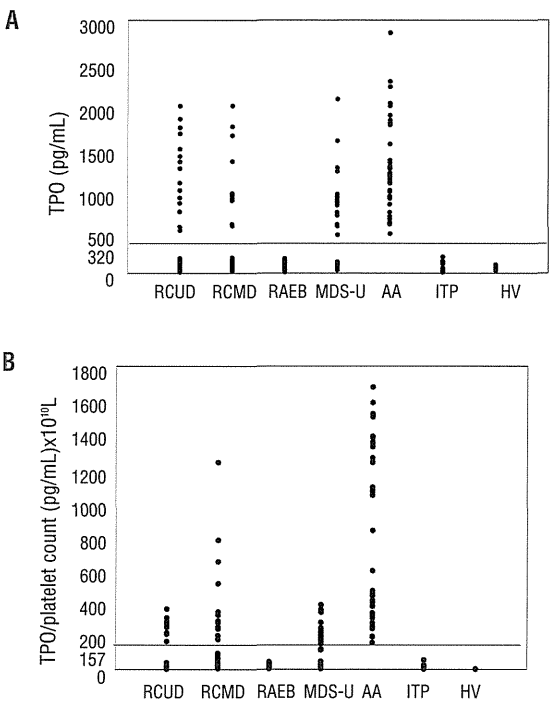

Figure 1. **Plasma thrombopoietin levels in patients with thrombocytopenia and healthy volunteers. (A) Plasma thrombopoietin (TPO) levels for each patient group. (B) Corrected TPO values for each patient group. The horizontal line in each figure represents the cut-off value that potentially separates benign and pre-leukemic bone marrow failure. RCUD: refractory cytopenia with unilineage dysplasia; RCMD: refractory cytopenia with multilineage dysplasia; RAEB: refractory anemia with excess of blasts; MDS-U: unclassified myelodysplastic syndromes; AA: aplastic anemia; ITP: immune thrombocytopenia; HV: healthy volunteers.**

Response of patients with MDS to IST

Forty-five TPO^{high} MDS patients were treated with IST. Sixteen patients (7 with RCUD and 9 with MDS-U) were treated with a combination of ATG and CsA, while 29 patients (9 with RCUD, 10 with RCMD, and 10 with MDS-U) were treated with CsA alone. Response rates to ATG+CsA and CsA were 81.2% and 85.3%, respectively. In contrast, 7 TPO^{low} patients received CsA monotherapy that produced only one case of improved anemia (from 5.4 g/dL to 8.1 g/dL). The cumulative rate of response to IST in TPO^{high} patients was significantly higher than that in TPO^{low} patients (P=0.002), (*Online Supplementary Figure S2A*), while there was no significant difference either between patients with or without increased GPI-AP- granulocytes (P=0.38), (*Online Supplementary Figure S2B*) or between TPO^{high} patients with or without increased GPI-AP$^-$ granulocytes (P=0.28), (*Online Supplementary Figure S2C*). ROC analysis revealed the threshold TPO level affecting the response to IST to be 286.7 pg/mL, with a sensitivity of 0.580 and a specificity of 0.850 (Figure 2B).

After 6-17 months of IST, TPO levels were measured again in 4 patients who achieved a platelet recovery above 100 x 10^9/L. The corrected TPO levels before and after IST were 718.7/14.2 pg/mL/10^{10} L, 266.8/10.8 pg/mL/10^{10} L, 330.6/8.75 pg/mL/10^{10} L, and 170.6 /8.8 pg/mL/10^{10} L.

Correlation of high TPO levels with the prognosis of patients with MDS

The 5-year overall survival rates for RCUD, RCMD, MDS-U, and RAEB patients were 53.6%, 50.8%, 53.1%, and 37.4%, respectively (Figure 4A). The 5-year progression-free survival (PFS) rates for RCUD, RCMD, and MDS-U patients were 60.9%, 60.6%, and 71.4%, respectively (Figure 4B). The 5-year PFS rates, defined as whichever came first between: a) time from the first day of diagnosis until progression to AML; or b) disease-related death, was significantly higher for TPO^{high} patients than TPO^{low} patients with RCUD (94.1% *vs.* 60.6%; P=0.03) or RCMD (100.0% *vs.* 44.4%; P=0.006), while there was no significant difference between the two groups in patients with MDS-U (82.3% *vs.* 80.0%; P=0.22, Figure 4C-E). An ROC analysis revealed the threshold TPO level affecting

Table 2. **Multivariate analysis of factors negatively affecting progression-free survival of patients with myelodysplastic syndrome.**

	Hazard ratio	P
TPO (pg/mL) <320 *vs.* ≥320	0.05	0.009
Age (years old) <60 *vs.* ≥60	1.87	0.262
Gender female *vs.* male	0.12	0.009
IPSS 0 *vs.* 0.5 and 1.0	0.34	0.158
Transfusion yes *vs.* no	1.21	0.752
Abnormal karyotype yes *vs.* no	0.93	0.916

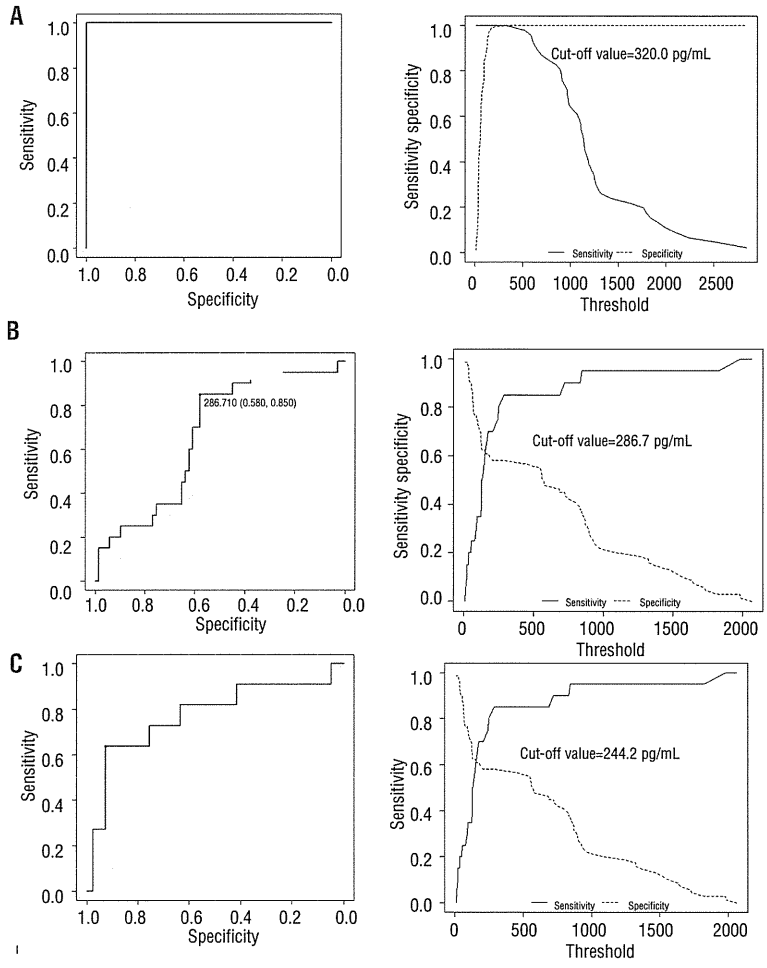

Figure 2. **Receiver operating characteristic (ROC) curves to determine thresholds of plasma TPO levels discriminating benign (aplastic anemia)/pre-leukemic BM failure (RAEB, A), response/no response to immunosuppressive therapy (IST, B), and progression/no progression to AML/death (C).**

progression to AML to be 244.2 pg/mL with a sensitivity of 0.927 and a specificity of 0.636 (Figure 2C). A multivariate analysis on patients with RCUD, RCMD and MDS-U revealed TPO^{low} and patient gender to be significant factors associated with progression to AML (Table 2). In contrast to previous analyses,[20] red blood cell transfusion requirements were not identified as a significant prognostic factor in this study cohort.

This may reflect the fact that we selected patients with thrombocytopenia. There was no significant difference in the percentages of patients requiring platelet transfusions among TPO^{high} (8/52, 4.3%) and TPO^{low} (2/46, 15.3%; P=0.09) patients. TPO levels were serially recorded for one patient as AA evolved into MDS-RAEB 20 months after IST. The TPO concentration was 1960 pg/mL at the onset of AA and 151 pg/mL when thrombocytopenia recurred with the emergence of atypical blasts in peripheral blood (*Online Supplementary Figure S3*).

Discussion

Consistent with previous reports, the present study revealed an increase in the TPO levels of patients with AA, a decrease in those with ITP, and relatively low TPO levels in patients with MDS.[13,14] While patients with RAEB had consistently low TPO levels, patients with low-risk MDS (RCUD, RCMD, and MDS-U) produced highly variable results. Feng *et al.* recently demonstrated similar variability among patients with hypoplastic MDS and reported the usefulness of TPO in distinguishing hypoplastic MDS from AA;[21] however, the significance of high TPO levels in a subset of patients with low-risk MDS was not the focus of the authors' attention. Our study is the first to demonstrate that a high concentration of TPO is associated with benign BM failure in patients with MDS as seen by the higher prevalence of increased GPI-AP$^-$ cells, lower incidence of clonal hematopoiesis, lower IPSS score, and better PFS in TPO^{high} patients compared to TPO^{low} patients. The negative prognostic impact of TPO levels below 320 pg/mL was confirmed by a multivariate analysis which also identified patient gender to be a poor prognostic factor as demonstrated by previous studies.[22,23] Plasma TPO levels are negatively regulated by platelets and megakaryocytes through their binding of TPO.[24,25] Some studies show an inverse correlation between TPO levels and BM megakaryocyte count,[26,27] but the TPO levels of patients with RAEB were consistently low in our study despite the low megakaryocyte content (*data not shown*). Low TPO levels in MDS patients with a poor prognosis may be

explained by an increased turnover of platelets produced by abnormal megakaryocytes.[28] We previously demonstrated that the aberrant increase in the proportion of immature platelets is frequently seen in MDS patients with chromosomal abnormalities associated with poor prognosis.[28] Increased production and destruction of platelets may accelerate TPO consumption in patients with RAEB, leading to a decrease in plasma TPO levels. Although one report demonstrated increased TPO receptors on the megakaryocytes of MDS patients using flow cytometry,[14] we were unable to reproduce their results (*data not shown*).

Small populations of GPI-AP$^-$ cells have been detected in a subset of patients with refractory anemia as defined by French-American-British classification and are associated with a favorable response to IST and good future prognosis.[2] Patients with increased GPI-AP$^-$ cells (PNH$^+$ patients) are characterized by predominant thrombocytopenia and no increase in BM megakaryocytes,[6,9] which agrees with our findings of high TPO levels in all PNH$^+$ patients with MDS and no PNH$^+$ patients with low TPO levels. These results show no need to examine peripheral blood for GPI-AP$^-$ cells in patients with BM failure if their TPO levels are less than 320 pg/mL.

The response rate to ATG+CsA therapy or CsA monotherapy for TPO^{high} MDS patients was as high as or higher than the response for AA patients.[29] When we previously assessed the efficacy of CsA therapy for patients with thrombocytopenia and decreased BM megakaryocytes, more than 70% improved regardless of the presence or absence of GPI-AP$^-$ cells (Seiki *et al.*, unpublished observation, 2013). High TPO levels may have a stronger association with the immune pathophysiology of BM failure in a subset of MDS than the presence of increased GPI-AP$^-$ cells. However, the impact of the increased percentage of GPI-AP$^-$ granulocytes on PFS could not be analyzed by our multivariate analysis because all patients with increased GPI-AP$^-$ granulocytes were sorted into the TPO^{high} group. When we conducted another multivariate analysis using increased GPI-AP$^-$ granulocytes, rather than TPO levels, as an independent factor, the hazard ratio of the increased GPI-AP$^-$ granulocytes was 0.64, with a *P* value of 0.69. Thus, the impact of increased GPI-AP$^-$ granulocytes on PFS appears to be much smaller than high TPO levels.

Previous reports documented the important role of DRB1*1501 as a predictor of response to IST in patients with MDS.[8] This factor may also have affected PFS in our patient cohort. Unfortunately, since only a limited number of patients underwent HLA typing, its impact on PFS could not be determined in this study. However, we previously examined various factors, including GPI-AP$^-$ cells and DRB1*1501, for their association with good response to IST in 140 patients with AA using multivariate analysis and found that only the presence of increased GPI-AP$^-$ cells significantly predicts favorable response to IST.[30,31] Thus, it is unlikely that DRB1*1501 affects PFS of patients with MDS more strongly than increased GPI-AP$^-$ cells or high TPO levels. Cytogenetic abnormality was not identified as a poor risk factor by the multivariate analysis. This is probably because 15 of 21 patients with cytogenetic abnormalities had del(13q), which represents benign BM failure with immune pathophysiology.[32]

Although the exact mechanism for decreased TPO in MDS patients with a poor prognosis remains unclear,

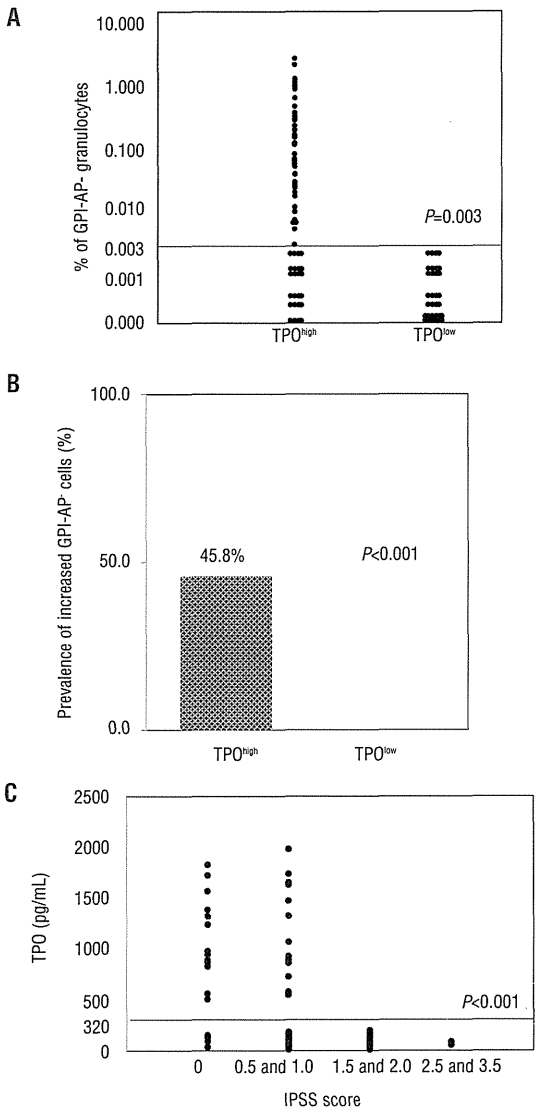

Figure 3. **Relationship between thrombopoietin levels and other prognostic markers for patients with myelodysplastic syndrome.** (A) Percentage of GPI-AP$^-$ granulocytes in TPO^{high} (n=55) and TPO^{low} (n=65) patients. The horizontal line represents the cut-off value that separates significant and non-significant increases in GPI-AP$^-$ granulocyte percentage. (B) The prevalence of increased GPI-AP$^-$ granulocytes and/or erythrocytes in TPO^{high} (n=55) and TPO^{low} (n=65) patients. (C) TPO levels for MDS patients classified by IPSS score. GPI-AP$^-$ cells, glycosylphosphatidylinositol-anchored protein-deficient cells; TPOhigh, thrombopoietin levels ≥320 pg/mL; TPO^{low}: thrombopoietin levels <320 pg/mL; RCMD: refractory cytopenia with multilineage dysplasia; MDS-U: unclassified MDS; AA: aplastic anemia; IPSS: International Prognostic Scoring System.

measurement of its concentration could play a significant role in managing MDS with thrombocytopenia. A patient with TPO levels of 320 pg/mL or over is considered to have a good prognosis with a small likelihood of developing AML, and IST can be considered rather than radical treatments such as chemotherapy and stem cell transplantation. Recent National Comprehensive Cancer Network guidelines recommend hypomethylating agents as a treatment for MDS patients with thrombocytopenia,[33] but this

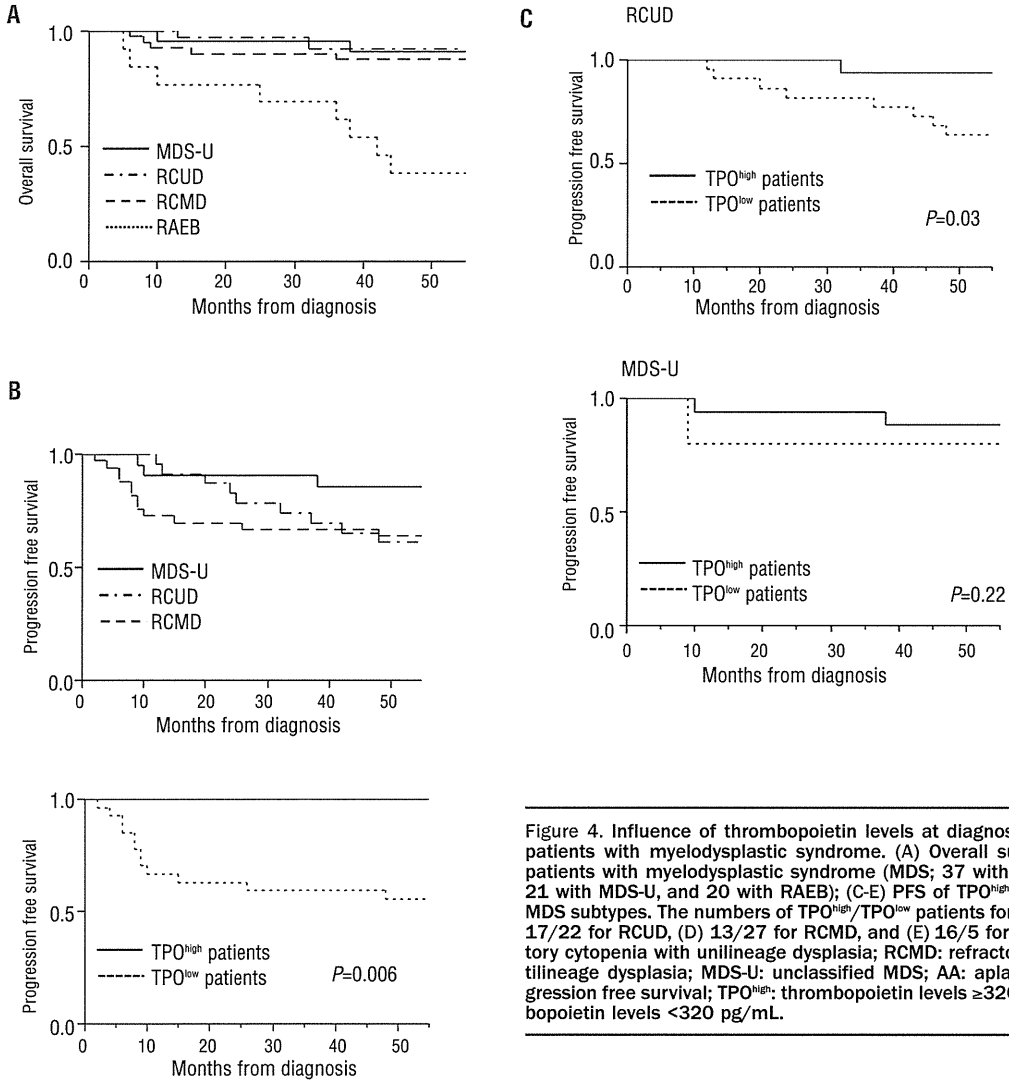

Figure 4. Influence of thrombopoietin levels at diagnosis on survival rates of patients with myelodysplastic syndrome. (A) Overall survival and (B) PFS of patients with myelodysplastic syndrome (MDS; 37 with RCUD, 40 with RCMD, 21 with MDS-U, and 20 with RAEB); (C-E) PFS of TPO^{high} and TPO^{low} patients by MDS subtypes. The numbers of TPO^{high}/TPO^{low} patients for each subtype were (C) 17/22 for RCUD, (D) 13/27 for RCMD, and (E) 16/5 for MDS-U. RCUD: refractory cytopenia with unilineage dysplasia; RCMD: refractory cytopenia with multilineage dysplasia; MDS-U: unclassified MDS; AA: aplastic anemia; PFS: progression free survival; TPO^{high}: thrombopoietin levels ≥320 pg/mL; TPO^{low}: thrombopoietin levels <320 pg/mL.

option may be hazardous to TPO^{high} patients because their BM failure is not based on abnormal stem cells with preleukemic features. Measurement of TPO levels is, therefore, recommended for patients with low-risk MDS and thrombocytopenia so that the most appropriate therapy can be chosen. The exact role of TPO levels in the management of MDS will need to be evaluated in a prospective study.

Acknowledgments

We are deeply indebted to Ms. Rie Ooumi for technical assistance and to the following physicians for providing patients' data: A. Urabe of NTT Kanto Hospital; T. Endo and T. Kondo of the Hokkaido University Hospital; Y. Kataoka of the Ikeda City Hospital; M. Kofune of the Sapporo Medical University Hospital; T. Ueki, D. Akabane and H. Kobayashi of Nagano Red Cross Hospital; A. Sawazaki of NTT Kanazawa Hospital; A. Matsuda of Saitama Medical School Hospital; H. Fuse of Matsudo City Hospital; M. Ueda of Ishikawa Prefectural Hospital; S. Yoshida of Miyazaki Prefectural Miyazaki Hospital; K. Wakasa of Aiiku Hospital; R. Matsuoka and K. Kawakami of Kagawa Prefectural Central Hospital; T. Masunari and T. Kiguchi of Chugoku Central Hospital; R. Imamura of Kurume University Hospital; S. Matano of Tonami General Hospital; T. Sekine of Matsuzaka Central Hospital; A.Nishiyama of Ichinomiya Municipal Hospital;M. Iino of Yamanashi Prefectural Central Hospital; M. Tai of Municipal Tsuruga Hospital; K.Yoshinaga of Tokyo Women's Medical University Hospital; N. Seno of Shinshu University Hospital; K. Ito of Ogawa Red Cross Hospital; M Masuya of Mie University Hospital; N. Aotsuka of Narita Red Cross Hospital; Y. Terasaki of Toyama City Hospital; T.Yoshida and T. Kurokawa of Toyama Prefectural Central Hospital.

Authorship and Disclosures

Information on authorship, contributions, and financial and other disclosures was provided by the authors and is available with the online version of this article at www.haematologica.org.

References

1. Sloand EM, Olnes MJ, Shenoy A, Weinstein B, Boss C, Loeliger K, et al. Alemtuzumab treatment of intermediate-1 myelodysplasia patients is associated with sustained improvement in blood counts and cytogenetic remissions. J Clin Oncol. 2010;28(35): 5166-73.
2. Wang H, Chuhjo T, Yasue S, Omine M, Nakao S. Clinical significance of a minor population of paroxysmal nocturnal hemoglobinuria-type cells in bone marrow failure syndrome. Blood. 2002;100(12):3897-902.
3. Ishikawa T, Tohyama K, Nakao S, Yoshida Y, Teramura M, Motoji T, et al. A prospective study of cyclosporine A treatment of patients with low-risk myelodysplastic syndrome: presence of CD55(-)CD59(-) blood cells predicts platelet response. Int J Hematol. 2007;86(2):150-7.
4. Kusumoto S, Jinnai I, Matsuda A, Murohashi I, Bessho M, Saito M, et al. Bone marrow patterns in patients with aplastic anaemia and myelodysplastic syndrome: observations with magnetic resonance imaging. Eur J Haematol. 1997;59(3):155-61.
5. Barrett J, Saunthararajah Y, Molldrem J. Myelodysplastic syndrome and aplastic anemia: distinct entities or diseases linked by a common pathophysiology? Semin Hematol. 2000;37(1):15-29.
6. Dunn DE, Tanawattanacharoen P, Boccuni P, Nagakura S, Green SW, Kirby MR, et al. Paroxysmal nocturnal hemoglobinuria cells in patients with bone marrow failure syndromes. Ann Intern Med. 1999;131(6):401-8.
7. Wang H, Chuhjo T, Yamazaki H, Shiobara S, Teramura M, Mizoguchi H, et al. Relative increase of granulocytes with a paroxysmal nocturnal haemoglobinuria phenotype in aplastic anaemia patients: the high prevalence at diagnosis. Eur J Haematol. 2001;66 (3):200-5.
8. Saunthararajah Y, Nakamura R, Wesley R, Wang QJ, Barrett AJ. A simple method to predict response to immunosuppressive therapy in patients with myelodysplastic syndrome. Blood. 2003;102(8):3025-7.
9. Sugimori C, Mochizuki K, Qi Z, Sugimori N, Ishiyama K, Kondo Y, et al. Origin and fate of blood cells deficient in glycosylphosphatidylinositol-anchored protein among patients with bone marrow failure. Br J Haematol. 2009;147(1):102-12.
10. Borowitz MJ, Craig FE, Digiuseppe JA, Illingworth AJ, Rosse W, Sutherland DR, et al. Guidelines for the diagnosis and monitoring of paroxysmal nocturnal hemoglobinuria and related disorders by flow cytometry. Cytometry B Clin Cytom. 2010;78(4): 211-30.
11. Emmons RV, Reid DM, Cohen RL, Meng G, Young NS, Dunbar CE, et al. Human thrombopoietin levels are high when thrombocytopenia is due to megakaryocyte deficiency and low when due to increased platelet destruction. Blood. 1996;87(10):4068-71.
12. Hou M, Andersson PO, Stockelberg D, Mellqvist UH, Ridell B, Wadenvik H. Plasma thrombopoietin levels in thrombocytopenic states: implication for a regulatory role of bone marrow megakaryocytes. Br J Haematol. 1998;101(3):420-4.
13. Ogata K, Tamura H. Thrombopoietin and myelodysplastic syndromes. Int J Hematol. 2000;72(2):173-7.
14. Tamura H, Ogata K, Luo S, Nakamura K, Yokose N, Dan K, et al. Plasma thrombopoietin (TPO) levels and expression of TPO receptor on platelets in patients with myelodysplastic syndromes. Br J Haematol. 1998;103(3):778-84.
15. Camitta BM, Doney K. Immunosuppressive therapy for aplastic anemia: indications, agents, mechanisms, and results. Am J Pediatr Hematol Oncol. 1990;12(4):411-24.
16. Parker C, Omine M, Richards S, Nishimura J, Bessler M, Ware R, et al. Diagnosis and management of paroxysmal nocturnal hemoglobinuria. Blood. 2005;106(12):3699-709.
17. Kulagin A, Golubovskaya I, Ganapiev A, Babenko E, Sipol A, Pronkina N, et al. Prognostic value of minor PNH clones in aplastic anaemia patients treated with ATG-based immunosuppression: results of a two-centre prospective study. Bone Marrow Transplantation. 2011;46:S83-S4.
18. Cheson BD, Greenberg PL, Bennett JM, Lowenberg B, Wijermans PW, Nimer SD, et al. Clinical application and proposal for modification of the International Working Group (IWG) response criteria in myelodysplasia. Blood. 2006;108(2):419-25.
19. Ishiyama K, Chuhjo T, Wang H, Yachie A, Omine M, Nakao S. Polyclonal hematopoiesis maintained in patients with bone marrow failure harboring a minor population of paroxysmal nocturnal hemoglobinuria-type cells. Blood. 2003;102(4):1211-6.
20. Malcovati L, Germing U, Kuendgen A, Della Porta MG, Pascutto C, Invernizzi R, et al. Time-dependent prognostic scoring system for predicting survival and leukemic evolution in myelodysplastic syndromes. J Clin Oncol. 2007;25(23):3503-10.
21. Feng XM, Scheinberg P, Wu CO, Samsel L, Nunez O, Prince C, et al. Cytokine signature profiles in acquired aplastic anemia and myelodysplastic syndromes. Haematologica. 2011;96(4):602-6.
22. Malcovati L, Porta MG, Pascutto C, Invernizzi R, Boni M, Travaglino E, et al. Prognostic factors and life expectancy in myelodysplastic syndromes classified according to WHO criteria: a basis for clinical decision making. J Clin Oncol. 2005;23(30):7594-603.
23. Nosslinger T, Tuchler H, Germing U, Sperr WR, Krieger O, Haase D, et al. Prognostic impact of age and gender in 897 untreated patients with primary myelodysplastic syndromes. Ann Oncol. 2010;21(1):120-5.
24. Nagasawa T, Hasegawa Y, Shimizu S, Kawashima Y, Nishimura S, Suzukawa K, et al. Serum thrombopoietin level is mainly regulated by megakaryocyte mass rather than platelet mass in human subjects. Br J Haematol. 1998;101(2):242-4.
25. Kaushansky K. Thrombopoietin: the primary regulator of megakaryocyte and platelet production. Thromb Haemost. 1995;74(1):521-5.
26. Nagata Y, Shozaki Y, Nagahisa H, Nagasawa T, Abe T, Todokoro K. Serum thrombopoietin level is not regulated by transcription but by the total counts of both megakaryocytes and platelets during thrombocytopenia and thrombocytosis. Thromb Haemost. 1997;77(5):808-14.
27. de Sauvage FJ, Carver-Moore K, Luoh SM, Ryan A, Dowd M, Eaton DL, et al. Physiological regulation of early and late stages of megakaryocytopoiesis by thrombopoietin. J Exp Med. 1996;183(2):651-6.
28. Sugimori N, Kondo Y, Shibayama M, Omote M, Takami A, Sugimori C, et al. Aberrant increase in the immature platelet fraction in patients with myelodysplastic syndrome: a marker of karyotypic abnormalities associated with poor prognosis. Eur J Haematol. 2009;82(1):54-60.
29. Bacigalupo A, Broccia G, Corda G, Arcese W, Carotenuto M, Gallamini A, et al. Antilymphocyte globulin, cyclosporin, and granulocyte colony-stimulating factor in patients with acquired severe aplastic anemia (SAA): a pilot study of the EBMT SAA Working Party. Blood. 1995;85(5):1348-53.
30. Sugimori C, Yamazaki H, Feng X, Mochizuki K, Kondo Y, Takami A, et al. Roles of DRB1 *1501 and DRB1 *1502 in the pathogenesis of aplastic anemia. Exp Hematol. 2007;35(1):13-20.
31. Sugimori C, Chuhjo T, Feng XM, Yamazaki H, Takami A, Teramura M, et al. Minor population of CD55(-)CD59(-) blood cells predicts response to immunosuppressive therapy and prognosis in patients with aplastic anemia. Blood. 2006;107(4):1308-14.
32. Hosokawa K, Katagiri T, Sugimori N, Ishiyama K, Sasaki Y, Seiki Y, et al. Favorable outcome of patients who have 13q deletion: a suggestion for revision of the WHO 'MDS-U' designation. Haematologica. 2012; 97(12):1845-9.
33. Greenberg PL, Attar E, Battiwalla M, Bennett JM, Bloomfield CD, DeCastro CM, et al. Myelodysplastic syndromes. J Natl Compr Canc Netw. 2008;6(9):902-26.

Immunity
Article

Monocyte-Derived Dendritic Cells Perform Hemophagocytosis to Fine-Tune Excessive Immune Responses

Hideaki Ohyagi,[1,10] Nobuyuki Onai,[2,3,10] Taku Sato,[2,3] Satoshi Yotsumoto,[2] Jiajia Liu,[1] Hisaya Akiba,[4] Hideo Yagita,[4] Koji Atarashi,[5] Kenya Honda,[5] Axel Roers,[6] Werner Müller,[7] Kazutaka Kurabayashi,[2] Mayuka Hosoi-Amaike,[2] Naoto Takahashi,[1] Makoto Hirokawa,[8] Kouji Matsushima,[3,9] Kenichi Sawada,[1] and Toshiaki Ohteki[2,3,*]
[1]Department of Hematology, Nephrology and Rheumatology, Akita University Graduate School of Medicine, Akita 010-8543, Japan
[2]Department of Biodefense Research, Medical Research Institute, Tokyo Medical and Dental University, Tokyo 113-8510, Japan
[3]Japan Science and Technology Agency, Core Research for Evolutional Science and Technology (CREST), Tokyo 102-0075, Japan
[4]Department of Immunology, Juntendo University School of Medicine, Tokyo 113-8421, Japan
[5]Department of Immunology, Graduate School of Medicine, The University of Tokyo, Tokyo 113-0033, Japan
[6]Institute for Immunology, University of Technology Dresden, Medical Faculty Carl-Gustav Carus, 01307 Dresden, Germany
[7]Faculty of Life Science, University of Manchester, Manchester M13 9PL, UK
[8]Clinical Oncology Center, Akita University Hospital, Akita 010-8543, Japan
[9]Department of Molecular Preventive Medicine, Graduate School of Medicine, The University of Tokyo, Tokyo 113-0033, Japan
[10]These authors contributed equally to this work
*Correspondence: ohteki.bre@mri.tmd.ac.jp
http://dx.doi.org/10.1016/j.immuni.2013.06.019

SUMMARY

Because immune responses simultaneously defend and injure the host, the immune system must be finely regulated to ensure the host's survival. Here, we have shown that when injected with high Toll-like receptor ligand doses or infected with lymphocytic choriomeningitis virus (LCMV) clone 13, which has a high viral turnover, inflammatory monocyte-derived dendritic cells (Mo-DCs) engulfed apoptotic erythroid cells. In this process, called hemophagocytosis, phosphatidylserine (PS) served as an "eat-me" signal. Type I interferons were necessary for both PS exposure on erythroid cells and the expression of PS receptors in the Mo-DCs. Importantly, hemophagocytosis was required for interleukin-10 (IL-10) production from Mo-DCs. Blocking hemophagocytosis or Mo-DC-derived IL-10 significantly increased cytotoxic T cell lymphocyte activity, tissue damage, and mortality in virus-infected hosts, suggesting that hemophagocytosis moderates immune responses to ensure the host's survival in vivo. This sheds light on the physiological relevance of hemophagocytosis in severe inflammatory and infectious diseases.

INTRODUCTION

An immune response is a two-edged sword that, while directly attacking a pathogen, simultaneously damages the body (Schneider and Ayres, 2008). In an infected host, dendritic cells (DCs) and other innate immune cells sense pathogens through receptors that detect pathogen-associated molecular patterns (PAMPs) or damage-associated molecular patterns (DAMPs). These danger signals trigger DC maturation and induce immunogenic DCs that produce inflammatory cytokines and activate both the innate and adaptive immune systems. The adaptive immune system eliminates the pathogen in an antigen (Ag)-specific manner and protects the host from reinfection (Medzhitov and Janeway, 1997; Banchereau et al., 2000; Cooper and Alder, 2006). However, infection-induced immune responses, particularly virus-specific cytotoxic T lymphocytes (CTLs), cytokines, and chemical mediators, simultaneously damage tissue (Clark, 2007; Lambeth, 2007; Rouse and Sehrawat, 2010). Therefore, immune responses require regulatory machinery to maintain the fine balance between defense and self-injury during infections; the more severe the infection, the greater the regulatory control must be. However, little attention has been paid to the nature of the machinery balancing these immune-response effects. This study focuses on hemophagocytosis, which is conventionally viewed as an indicator of severe inflammation, and identifies DC-mediated hemophagocytosis as the machinery that fine-tunes immune responses and ensures host survival under severe inflammatory and infectious conditions.

RESULTS

Toll-like Receptor Ligands Induce Hemophagocytosis

Pattern recognition receptors (PRRs), including Toll-like receptors (TLRs) and nucleotide oligomerization domain (NOD)-like receptors (NLRs), sense microbial infection and mediate immune and inflammatory responses (Kawai and Akira, 2010). In this study, we found that high doses (~200 μg) of various TLR and NLR ligands injected into wild-type (WT) mice induced hemophagocytosis, an indicator of severe inflammatory conditions such as hemophagocytic syndrome (Larroche and Mouthon, 2004; Janka, 2007; Maakaroun et al., 2010). Hemophagocytosis, typically defined as the engulfment of TER119$^+$ erythroid cells by CD11c$^+$ cells, was detected by the presence of CD11c$^+$TER119$^+$ cells in the peripheral blood. Of the ligands used, unmethylated CpG DNA (CpG) and poly I:C induced hemophagocytosis in

the peripheral blood most efficiently (Figure 1A). After injecting CpG, the number of $CD11c^+TER119^+$ cells in the peripheral blood increased according to the CpG dosage, peaking 18 hr later in the bone marrow (BM) and peripheral blood and 3 days afterward in the spleen (see Figures S1A–S1D available online). This suggested that hemophagocytosis in the peripheral blood correlated well with and reflected that in the BM. Sorted $CD11c^+$ $TER119^+$ cells displayed typical hemophagocytosis with both attached and internalized erythroid cells by Diff-Quick stain and electron microscopic analysis (Figures 1B and 1C). CpG also induced other criteria of hemophagocytic syndrome, including fever, splenomegaly, cytopenia (evaluated by the reduction of hemoglobin and platelets), and hypertriglyceridemia (Figures S1E–S1I). We used a recently reported protocol (Zoller et al., 2011) to further confirm the intracellular localization of erythroid cells inside $CD11c^+$ cells. In brief, TER119 exposed on $CD11c^+$ cell surfaces was blocked with saturating amounts of an unlabeled antibody (Ab) against TER119 and then stained with an anti-TER119 Ab. As expected, intracellular TER119 was stained after permeabilization in a CpG dose-dependent manner (Figure S1J). These results clearly demonstrated the intracellular localization of erythroid cells and correlated well with those of $CD11c^+TER119^+$ staining without permeabilization (Figure S1D). This is reasonable because hemophagocytosis is a sequential event: apoptotic erythroid cells expressing phosphatidylserine (PS) are initially attached to PS receptors on the $CD11c^+$ cells and then are gradually phagocytosed into the cells.

Hemophagocytosing DCs Are of Monocyte Origin

The phenotype of the hemophagocytosing $CD11c^+$ cells was major histocompatibility complex (MHC) class $II^{lo}CD11b^{hi}F4/80^+Gr\text{-}1^{hi}CD40^-CD80^{hi}CD86^-$ (Figure 1D). This is characteristic of inflammatory monocyte-derived DCs (Mo-DCs), which are induced under inflammatory conditions (Randolph et al., 1999; León et al., 2007; Serbina et al., 2008; Auffray et al., 2009; Geissmann et al., 2010). To confirm the Mo-DCs' origin, we sorted inflammatory monocytes, defined as $Ly6c^{hi}CX_3CR1^{int}CD11b^+$ $CD11c^-$ cells, from the BM of $Cx_3cr1^{GFP/+}$ mice ($CD45.1^-$ $CD45.2^+$), which expressed EGFP under the endogenous *Cx3cr1* locus (Jung et al., 2000) (Figure S2A). We injected these cells into WT mice ($CD45.1^+CD45.2^-$) and then injected CpG. After 18 hr, the transferred inflammatory monocytes had become $CD11c^+$, and approximately 40% were engulfing $TER119^+$ cells (Figures 1E and 1F). In $Cx_3cr1^{GFP/+}$ mice injected directly with CpG, the hemophagocytes consisted mostly of $Ly6c^{hi}CX_3CR1^{int}$ inflammatory monocyte-derived DCs (Figure S2B), indicating that inflammatory monocytes were the major hemophagocyte precursor. During infection and inflammation, inflammatory monocytes mobilize from the BM to the periphery CCR2 dependently (Boring et al., 1997; Serbina and Pamer, 2006). Because CpG-induced hemophagocytosis is mediated by Mo-DCs, we conducted experiments with $Ccr2^{-/-}$ mice, in which circulating monocytes are able to leave the BM but inflammatory monocytes cannot. In WT mice, serum amounts of the CCR2 ligands CCL2, CCL7, and CCL12 peaked 3–6 hr after CpG injection (Figures 2A–2C); CCR2 was predominantly expressed on $Ly6c^{hi}$ inflammatory monocytes and to a lesser extent on $CD11c^+$ $TER119^+$ cells (Figure 2D). Importantly, the percentage of peripheral blood $CD11c^+TER119^+$ cells after CpG injection was greatly reduced in the $Ccr2^{-/-}$ mice (Boring et al., 1997), partially reduced in $Ccl2^{-/-}$ mice (Lu et al., 1998)—probably due to CCL7 and CCL12, which are also CCR2 ligands—and unaffected in $Cx_3cr1^{GFP/GFP}$ mice (Figure 2E). In contrast, the BM $CD11c^+TER119^+$ cell numbers after CpG injection were comparable between the WT and $Ccr2^{-/-}$ mice (Figure 2F). Collectively, these results demonstrate that CpG injection causes inflammatory monocytes to mobilize to the periphery, differentiate into Mo-DCs, and engulf mainly erythroid cells.

Involvement of "Find Me" and "Eat Me" Signals in TLR Ligand-Induced Hemophagocytosis

Cells undergoing apoptosis release "find me" signals to recruit phagocytes and expose PS, which is recognized by phagocytes as an "eat me" signal, on their surface (Nagata et al., 2010; Martin et al., 1996). PS is recognized directly by T cell immunoglobulin- and mucin-domain-containing (Tim)-1 and -4 and indirectly by the $\alpha_V\beta_3$ and $\alpha_V\beta_5$ integrins through milk-fat globule epidermal growth factor (EGF) factor 8 (MFG-E8), and by Tyro3, Axl, and Mer (TAM) family members through Gas6 and protein S (Martin et al., 1996; Hanayama et al., 2002; Kobayashi et al., 2007; Miyanishi et al., 2007; Nakayama et al., 2009). We next examined the roles of "find me" and "eat me" signals in CpG-induced hemophagocytosis. Serum amounts of ATP, recently identified as a "find me" signal (Elliott et al., 2009), increased rapidly after CpG injection, peaking 6 hr later (Figure 3A). The ATP receptor P2Y2 was predominantly expressed on $Ly6c^{hi}$ inflammatory monocytes, on BMDCs, and on Mo-DCs performing hemophagocytosis ($CD11c^+TER119^+$), but not on T or B cells (Figure 3B), suggesting that ATP is an important "find me" signal in hemophagocytosis. Indeed, injecting suramin, a competitive inhibitor of ATP-P2Y2 binding, effectively blocked the CpG-induced hemophagocytosis (Figure 3C).

Next, we examined the role of the "eat me" signal in CpG-induced hemophagocytosis. The number of apoptotic erythroid cells expressing PS, defined as annexin $V^+TER119^+$ cells, peaked 2–4 hr after CpG injection (Figure 3D). In this context, most of the apoptotic cells were $TER119^+$ erythroid cells, and some apoptotic $Gr\text{-}1^{hi}Ly6c^+$ granulocytes were also detected (Figures S3A–S3C). CpG-induced Mo-DCs were the major phagocytes for $TER119^+$ erythroid cells (data not shown). As "eat me" signal receptors, the Mo-DCs expressed Tim1, Tim4, and α_V and β_3 integrin (Figure 3E), and an injection of neutralizing Abs against "eat me" signal receptors significantly blocked hemophagocytosis (Figure 3F). CpG injection induced the production of the representative regulatory cytokine interleukin-10 (IL-10) in the peripheral blood at rates that increased with CpG dosage (Figure 3G), and this correlated well with hemophagocytosis (Figure S1D). Consistent with these results, excessive CpG stimulation triggers DC IL-10 production (Waibler et al., 2008). Of note, injecting PS receptor-neutralizing Abs, which prevents hemophagocytosis, significantly reduced the IL-10 production (Figure 3G). Injecting a high dose of poly I:C into WT mice produced similar results, with Mo-DCs (Figure S3D) and "find me" and "eat me" signals playing critical roles in the poly I:C-induced hemophagocytosis and accompanying IL-10 production (Figures S3E–S3G). Collectively, these results suggest that "find me" and "eat me" signals are critical for CpG-induced hemophagocytosis and that high CpG doses induce IL-10 production.

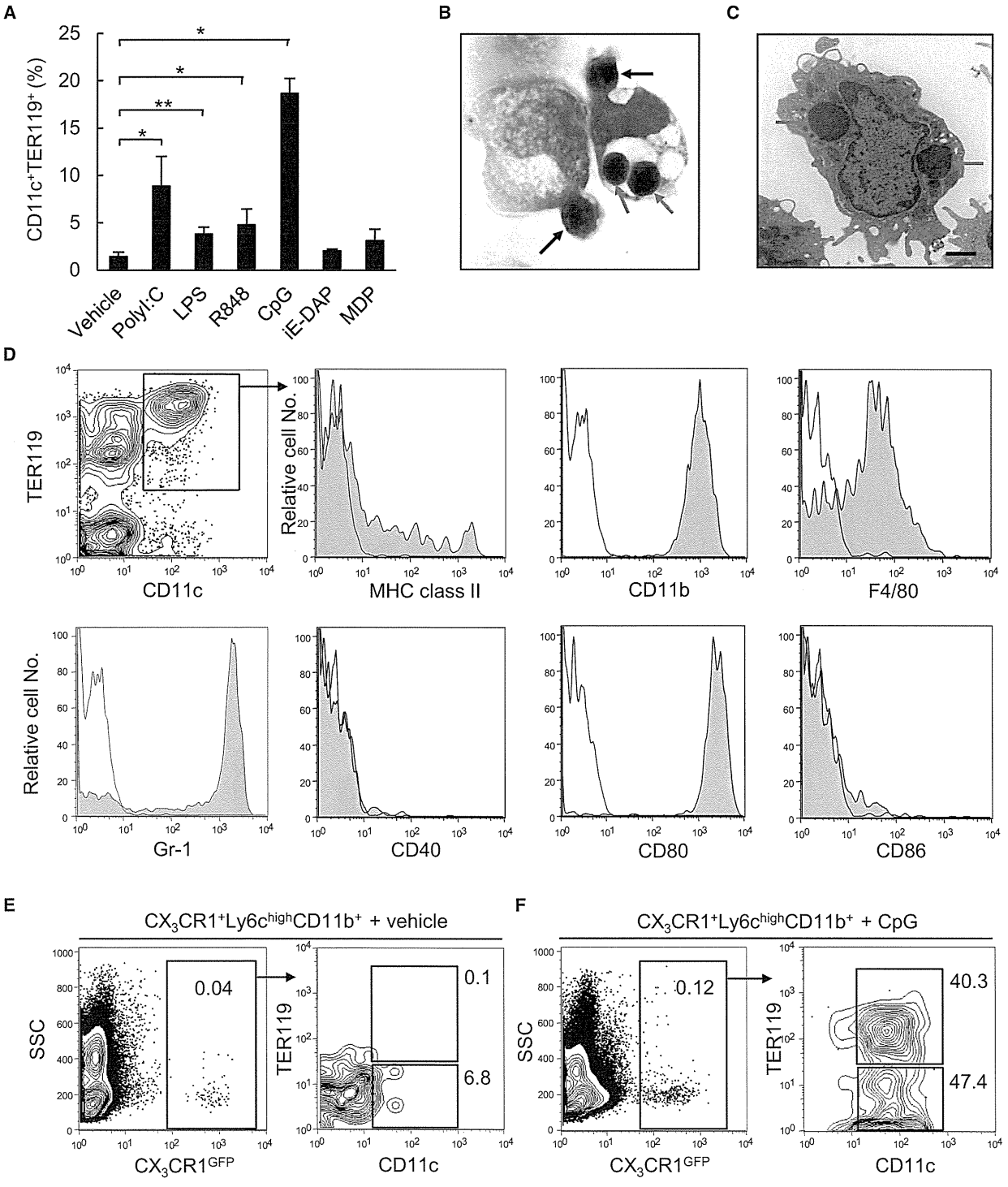

Figure 1. TLR Ligands Induce Hemophagocytosis

(A) Hemophagocytosis (%) in the peripheral blood of WT mice 18 hr after an injection of PBS (vehicle) or the indicated TLR or NLR ligand.

(B) Sorted CD11c$^+$TER119$^+$ cells from the BM of CpG-injected mice were stained with Diff-Quick. Red and black arrows indicate hemophagocytosed and attached erythroid cells, respectively. Original magnification was ×100.

(C) Sorted CD11c$^+$TER119$^+$ cells from the peripheral blood of CpG injected mice were analyzed by electron microscope. Scale bar represents 1 μm. Arrows indicate hemophagocytosed erythroid cells.

(legend continued on next page)

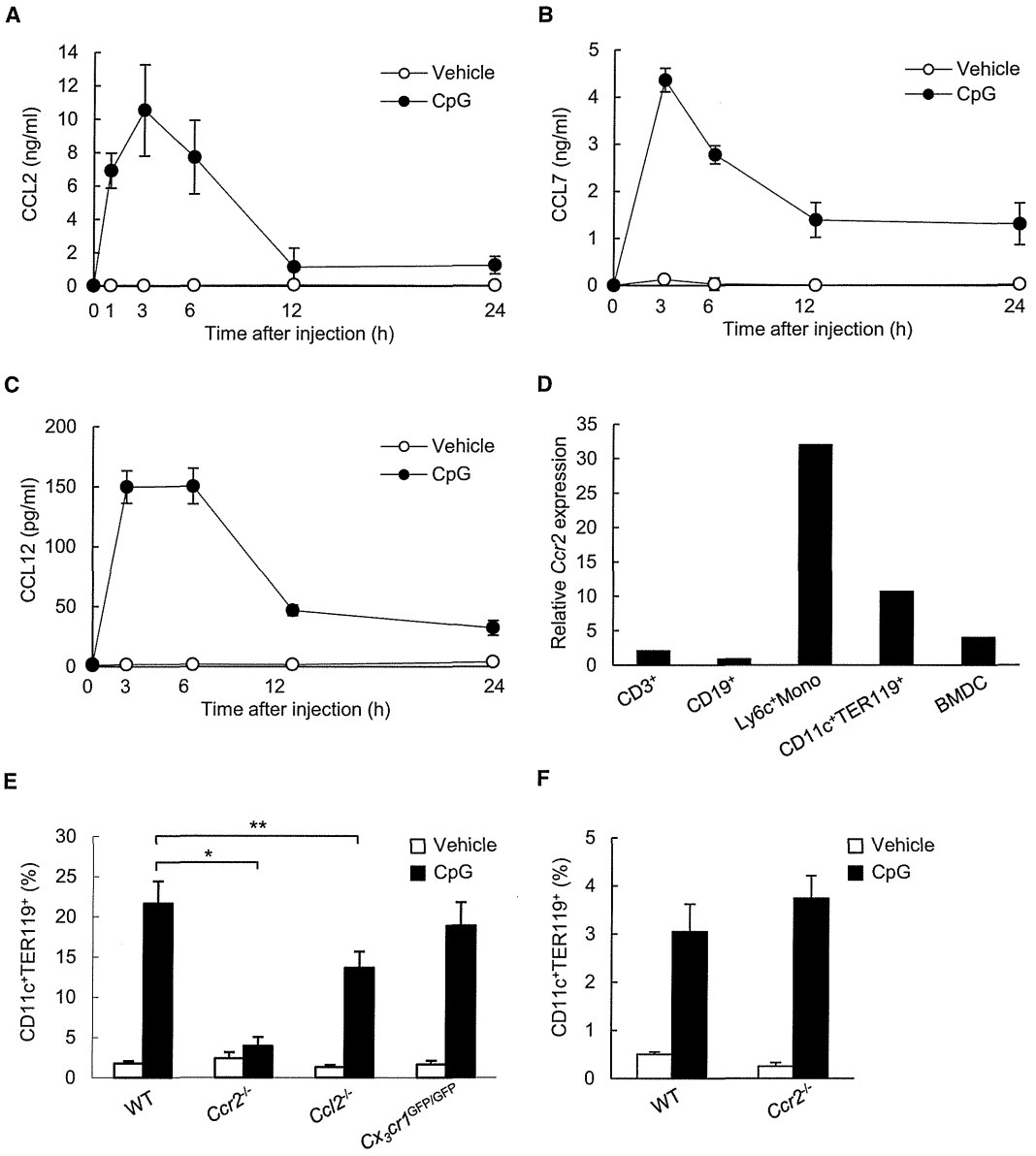

Figure 2. CCR2 Is Involved in Developing CpG-Induced Hemophagocytosis

(A–C) Kinetics of serum CCL2 (A), CCL7 (B), and CCL12 (C) production in WT mice after 200-μg CpG injection.

(D) Relative *Ccr2* mRNA expression in the indicated cell populations from WT mice 18 hr after 200-μg CpG injection. BMDC, bone marrow-derived DCs.

(E and F) Percentage of $CD11c^+TER119^+$ cells in the peripheral blood (E) and BM (F) of the indicated mice 18 hr after 200 μg CpG injection. Data represent the mean ± SD of three independent experiments. *$p < 0.01$, **$p < 0.05$. See also Figure S2.

Type I Interferon Signaling Is Essential in Virus-Induced Hemophagocytosis

On the basis of these findings, we examined the induction mechanism and physiological relevance of hemophagocytosis in virus infection. We used the lymphocytic choriomeningitis virus (LCMV) variant clone 13 (C13), which elicits a chronic infection (Matloubian et al., 1990), for two reasons. First, compared with the original LCMV Armstrong (Arm), C13 binds and infects DCs

(D) Cell-surface staining of $CD11c^+TER119^+$ cells in the peripheral blood of 200 μg CpG-injected WT mice after blocking with an unlabeled anti-TER119 Ab.

(E and F) Analysis of the peripheral blood progeny of BM inflammatory monocytes 18 hr after vehicle (E) or 200 μg CpG (F) injection. BM inflammatory monocytes ($CX_3CR1^{GFP/int}Ly6c^{hi}CD11b^+CD11c^-$, $CD45.2^+$, 1×10^6) were transplanted into WT mice ($CD45.1^+$). Data represent the mean ± SD of three independent experiments. *$p < 0.01$ and **$p < 0.05$. See also Figure S1.

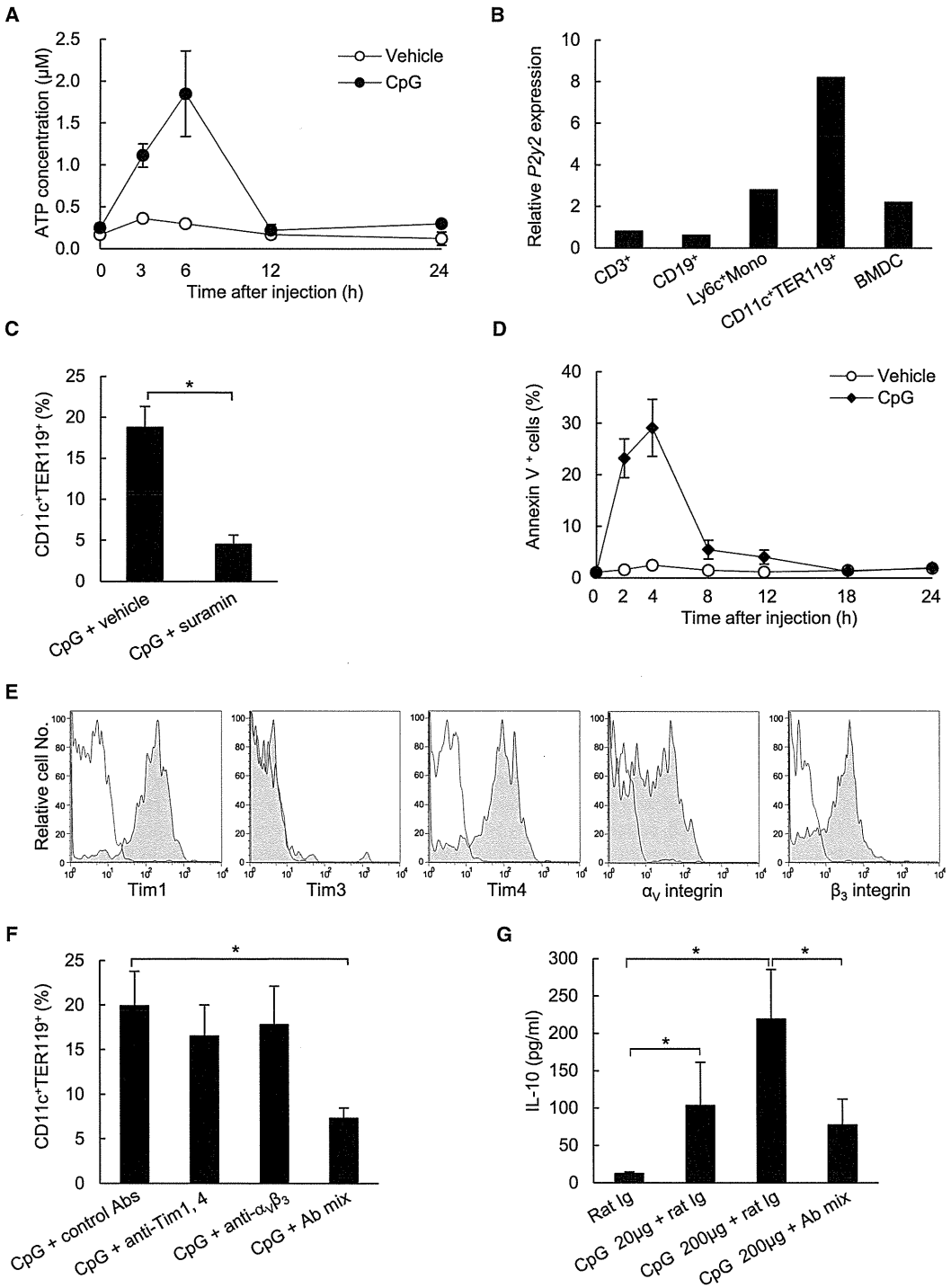

Figure 3. "Find Me" and "Eat Me" Signals in CpG-Induced Hemophagocytosis

(A) Serum ATP amount over time in WT mice after 200 μg CpG injection.

(B) Relative *P2y2* mRNA expression in CD11c$^+$TER119$^+$ cells from the peripheral blood and the indicated BM-derived cell populations 18 hr after 200 μg CpG injection.

(C) Percentage of CD11c$^+$TER119$^+$ cells in the peripheral blood of WT mice 18 hr after 200 μg CpG injection with 6 mg suramin.

(D) Percentage of annexin V$^+$ cells among TER119$^+$ cells in the peripheral blood of WT mice over time after PBS (vehicle) or 200 μg CpG injection.

(E) Expression of "eat me" signal receptors on CpG-induced CD11c$^+$TER119$^+$ cells. Shaded histograms represent cells stained with mAbs for the indicated molecules, and open histograms show labeling with isotype controls.

(legend continued on next page)

with high affinity, and it proliferates vigorously owing to two amino acid changes in its glycoprotein and polymerase, resulting in remarkably high viral nucleic acid amounts in vivo (Sevilla et al., 2000), possibly mimicking the effect of high-dose CpG or poly I:C injection. In this context, we expected that the more severe the infection, the more closely regulated the response. Second, most viruses that induce hemophagocytosis produce a chronic infection in humans (Clark 2007; Lambeth, 2007; Rouse and Sehrawat, 2010), although the role of hemophagocytosis in chronic infection is unknown. Indeed, the mRNA amounts for viral glycoprotein (GP) and nucleoprotein (NP) in C13-infected cells were remarkably higher than in Arm-infected cells, and we found that inflammatory monocytes, which are Mo-DC precursors, were a major C13 infection target (Figure S4A). As expected from these results, hemophagocytosis was induced more efficiently in C13-infected WT mice than in Arm-infected WT mice (Figure S4B); the intracellular localization of erythroid cells was again confirmed with the Diff-Quick staining and recently reported protocol (Zoller et al., 2011) (Figure S4C; data not shown). As with CpG injection, most of the apoptotic cells were TER119$^+$ erythroid cells and some were apoptotic Gr-1^{hi}Ly6c$^+$ granulocytes, suggesting that the contribution of apoptotic granulocytes was not negligible but relatively low (Figures S4D–S4F). In contrast, lymphocyte populations, including T, B, and NK cells, rarely became apoptotic at the same time point after C13 infection.

C13 infection induced type I interferon (IFN) production (Figures 4A and 4B). Interestingly, C13 infection-induced hemophagocytosis was significantly reduced in mice deficient for interferon-α receptor 1 (IFNAR1), a component of the type I IFN-receptor (Figures 4C and 4D). Consistent with these results, C13 infection in *Ifnar1*$^{-/-}$ mice severely impaired the PS exposure on erythroid cells and the Tim-1, Tim-4, and α_V and β_3 integrin expression on Mo-DCs (Figures 4E–4G), suggesting that type I IFNs are essential both for inducing PS on erythroid cells and for the development of Mo-DCs that express PS receptors. Indeed, ex vivo IFN-α stimulation directly induced the apoptosis of TER119$^+$ erythroid cells and, to a lesser extent, Gr-1^{hi}Ly6c$^+$ granulocytes (Figure S4G). In addition, IFN-α stimulation directly induced expression of PS receptors, i.e., Tim-1, Tim-4, and α_V and β_3 integrin, on inflammatory monocytes, precursors of Mo-DCs (Figures S4H and S4I). These results suggested that type I IFNs were necessary for both PS exposure on erythroid cells and the expression of PS receptors on the Mo-DCs.

Hemophagocytes Are the Major Source of IL-10

Finally, we examined the physiological relevance of hemophagocytosis in C13 infection. As expected from our findings thus far, injecting neutralizing Abs against Tim-1, Tim-4, and $\alpha_V\beta_3$ into C13-infected WT mice significantly suppressed hemophagocytosis (Figure 5A). Milk-fat globule epidermal growth factor 8 (MFG-E8) contains a PS-binding domain and an arginine-glycine-aspartate (RGD) motif, which binds to both $\alpha_V\beta_3$ and $\alpha_V\beta_5$ integrin on phagocytic cells, and it mediates the integrin-dependent engulfment of apoptotic cells and subsequent signaling (Hanayama et al., 2002; Akakura et al., 2003). As expected, *Mfge8* was clearly expressed in both inflammatory monocytes, a precursor of Mo-DCs, and Mo-DCs performing hemophagocytosis, whereas expression of other PS receptors including *Bai1*, *Stab2*, *Tyro3*, *Axl*, *Mertk*, *Gas6* detected by qPCR (Figure S5A) and Stabilin-2, Tyro-3, Axl, MerTK by specific Ab staining (Figure S5B) was minimal, suggesting that these molecules are unlikely involved in the uptake of apoptotic erythroid cells by Mo-DCs. Serum amounts of IL-10 and transforming growth factor β1 (TGF-β1), both of which suppress immune responses, increased after C13 infection, peaking at 24 hr (Figure 5B; data not shown). In line with our findings, C13 infection induces IL-10, contributing to the virus persistence in vivo (Brooks et al., 2006), although the mechanism of IL-10 production remains unknown. Importantly, injecting Abs against the Mo-DC PS receptors, which block hemophagocytosis, effectively reduced the IL-10 and TGF-β1 production (Figure 5B), whereas injecting IL-10-neutralizing Abs into WT mice did not suppress hemophagocytosis (Figure 5A). This suggests that the IL-10 production from Mo-DCs in response to C13 infection is hemophagocytosis-dependent. In this context, blocking IL-10 activity substantially reduced the TGF-β1 serum amounts, implying that IL-10 somehow regulates TGF-β1 production in C13-infected WT mice (Figure 5B). In the peripheral blood of C13-infected *Il10*^{Venus} reporter mice (Atarashi et al., 2011), IL-10 was expressed predominantly in CD11c$^+$TER119$^+$ cells and not in T cells (Figure 5C), and the absolute number of IL-10^{Venus+} CD11c^{+-} TER119$^+$ cells was much greater than that of IL-10^{Venus+} cells belonging to other populations, including CD11c$^+$TER119$^-$ cells (Figure 5D). This clearly demonstrates that hemophagocytes are the major source of IL-10 at an early phase of infection in vivo.

To further examine the IL-10 production machinery from Mo-DCs in response to C13 infection, we established ex vivo hemophagocytosis assay system, in which TER119$^-$ Mo-DCs and TER119$^+$ erythroid cells, separately sorted from the BM of C13-infected WT mice, were cocultured (Figure 6A). Of note, the erythroid cells were pHrodo-labeled prior to the coculture, which allowed the erythroid cells transported into lysosomes upon hemophagocytosis to be detected by their increased light emission under the acidic conditions. Consistent with the in vivo results, hemophagocytosis was clearly induced ex vivo (Figure 6A, left panel, 6B, and 6C). Most importantly, ex vivo blockage of hemophagocytosis with Abs against the Mo-DC's PS receptor impaired Mo-DC-derived IL-10 production (Figure 6A, right panel, 6D, and 6E). In this context, adding blocking Abs against Tim-1 and Tim-4 did not affect IL-10 production, whereas blocking Abs against integrin $\alpha_V\beta_3$ or $\alpha_V\beta_5$ significantly reduced the amount of IL-10 production (Figure 6E). In addition, neither blocking internalization of apoptotic erythroid cells with cytochalasin D nor opsonization of them induced Mo-DC-derived IL-10 production (Figure 6E). These results collectively demonstrated that IL-10 production from Mo-DCs is largely dependent on the integrin-mediated signals. Similar results

(F) Impaired CpG-induced hemophagocytosis in the peripheral blood of WT mice treated with blocking antibodies against Tim1, Tim4, $\alpha_V\beta_3$. The proportion of CD11c$^+$TER119$^+$ cells 18 hr after 200 μg CpG injection with isotype control Ab cocktails (500 μg each) or the indicated antibody mixtures (500 μg each). Ab mix, mixture of antibodies against Tim1, Tim4, $\alpha_V\beta_3$.

(G) IL-10 serum amounts 24 hr after the indicated treatments. Data represent the mean ± SD of three independent experiments. *$p < 0.01$. See also Figure S3.